Science of the Total Environment 842 (2022) 156631

Contents lists available at ScienceDirect

Science of the Total Environment

journal homepage: www.elsevier.com/locate/scitotenv

Antimony release and volatilization from rice paddy soils: Field and microcosm study

Jaime N. Caplette [a], L. Gfeller [a], D. Lei [b], J. Liao [b], J. Xia [b], H. Zhang [b], X. Feng [b,*], A. Mestrot [a,*]

[a] Institute of Geography, University of Bern, Switzerland
[b] State Key Laboratory of Environmental Geochemistry, Institute of Geochemistry, Chinese Academy of Sciences, PR China

HIGHLIGHTS

- Field and microcosm (flooded, ± manured) study of Sb release and volatilization.
- First quantitative field measurements of volatile Sb from rice paddy soils.
- Manuring microcosms did not impact Sb release, but produced more volatile Sb.
- Flooding microcosms induced rapid, temporary, Sb release that decreased with SO_4^{2-}.
- Volatile Sb in microcosms was correlated with surface water Sb concentrations.

GRAPHICAL ABSTRACT

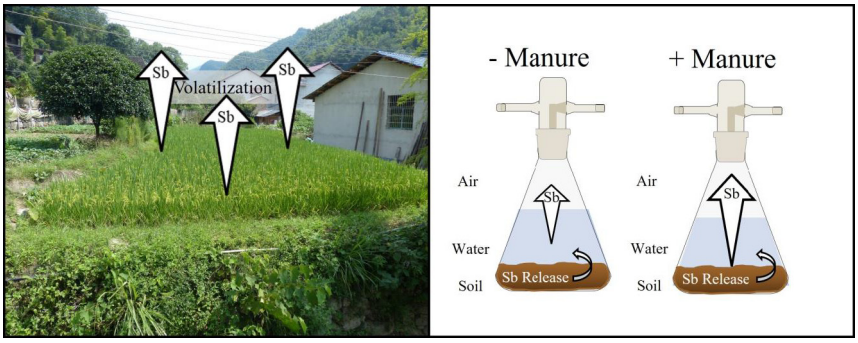

ARTICLE INFO

Editor: Filip M.G. Tack

Keywords:
Rice paddy
Xikuangshan
Manure
Sulfate reduction
Volatile antimony
Flooding

ABSTRACT

The fate of antimony (Sb) in submerged soils and the impact of common agricultural practices (e.g., manuring) on Sb release and volatilization is understudied. We investigated porewater Sb release and volatilization in the field and laboratory for three rice paddy soils. In the field study, the porewater Sb concentration (up to 107.1 μg L^{-1}) was associated with iron (Fe) at two sites, and with pH, Fe, manganese (Mn), and sulfate (SO_4^{2-}) at one site. The surface water Sb concentrations (up to 495.3 ± 113.7 μg L^{-1}) were up to 99 times higher than the regulatory values indicating a potential risk to aquaculture and rice agriculture. For the first time, volatile Sb was detected in rice paddy fields using a validated quantitative method (18.1 ± 5.2 to 217.9 ± 160.7 mg ha^{-1} y^{-1}). We also investigated the influence of two common rice agriculture practices (flooding and manuring) on Sb release and volatilization in a 56-day microcosm experiment using the same soils from the field campaign. Flooding induced an immediate, but temporary, Sb release into the porewater that declined with SO_4^{2-}, indicating that SO_4^{2-} reduction may reduce porewater Sb concentrations. A secondary Sb release, corresponding to Fe reduction in the porewater, was observed in some of the microcosms. Our results suggest flooding-induced Sb release into rice paddy porewaters is temporary but relevant. Manuring the soils did not impact the porewater Sb concentration but did enhance Sb volatilization. Volatile Sb (159.6 ± 108.4 to 2237.5 ± 679.7 ng kg^{-1} y^{-1}) was detected in most of the treatments and was correlated with the surface water Sb concentration. Our study indicates that Sb volatilization could be occurring at the soil-water interface or directly in the surface water and highlights that future works should investigate this potentially relevant mechanism.

* Corresponding authors.
E-mail addresses: fengxinbin@vip.skleg.cn (X. Feng), adrien.mestrot@giub.unibe.ch (A. Mestrot).

http://dx.doi.org/10.1016/j.scitotenv.2022.156631
Received 14 April 2022; Received in revised form 1 June 2022; Accepted 7 June 2022
Available online 9 June 2022

1. Introduction

Antimony (Sb) is classified as a priority pollutant of interest by the EU and the US-EPA (CEC, 1998). The World Health Organization recommends Sb concentration to be below 20 μg L^{-1} in drinking water (WHO, 2003). Major sources of Sb contamination in soils, sediments, and waters are ammunition (e.g., shooting ranges), mining, smelting, and coal combustion activities, and the manufacturing of electronic and industrial materials (Belzile et al., 2011; Filella et al., 2002; Okkenhaug et al., 2012). In aerobic environments, inorganic Sb is present as the pentavalent species, antimonate ($Sb(OH)_6^-$). In anaerobic environments, the trivalent species, antimonite ($Sb(OH)_3$) is dominant. Over a broad pH range, $Sb(OH)_3$ binds stronger with Fe- and Mn-oxyhydroxides (Guo et al., 2014; Leuz et al., 2006; Muller et al., 2015) and is less mobile than the geochemically similar arsenite ($As(OH)_3$), whereas the adsorption of $Sb(OH)_6^-$ is stronger when the pH is below 7 (Leuz et al., 2006; Muller et al., 2015).

Sinks for Sb in the aerobic environment are amorphous and crystalline Fe^{III} and Mn^{IV}- (oxy)hydroxides (Burton et al., 2019; Nriagu et al., 2007; Shangguan et al., 2016; Tighe et al., 2005; Vithanage et al., 2013; Xu et al., 2017). Soil anoxia caused by, for example, waterlogging facilitates microbially-mediated Fe^{III} and Mn^{IV} reduction and the release of bound Sb (Burton et al., 2014; Hockmann et al., 2014b; Okkenhaug et al., 2012; Yamaguchi et al., 2011). In reduced porewaters, Sb concentrations can decrease when Sb^V is reduced to Sb^{III} and subsequently re-adsorbed to the solid phase (Hockmann et al., 2015; Leuz et al., 2006; Tandy et al., 2018) or by the structural incorporation and/or co-precipitation of Sb with crystalline authigenic Fe phases (Burton et al., 2019; Hockmann et al., 2021; Karimian et al., 2019a, 2019b; Mitsunobu et al., 2010).

Biogenic reduced sulfur species can immobilize metal(loid)s by forming authigenic sulfides, for example, mackinawite, pyrite, amorphous iron sulfides (FeS_2), and meta-stibnite (Sb_2S_3) (Bennett et al., 2017; Burton et al., 2014; Hockmann et al., 2020; Liamleam and Annachhatre, 2007; Polack et al., 2009). The role of microbial sulfate reduction on Sb release in the environment has only been investigated in a few studies (Arsic et al., 2018; Bennett et al., 2017; Chen et al., 2003; Polack et al., 2009). During the initial stages of Fe-oxide sulfidization, Hockmann et al. (2020) showed Sb^V was released by sulfur-induced Fe-oxide dissolution. In low sulfide treatments, Sb^V was subsequently immobilized by sorption and structural incorporation into secondary Fe-oxides (Hockmann et al., 2020). In high sulfide treatments, 20 to 40 % of Sb^V was reduced to Sb^{III} and coordinated with O and S (Hockmann et al., 2020). Sb^{III} may be immobilized by binding with sulfide phases and the reduced sulfur groups on organic carbon in anoxic sediments (Arsic et al., 2018; Besold et al., 2019a, 2019b). Contrary to this, Sb complexing with biogenic sulfide may also increase Sb mobility in sediments by forming thio-antimonate (Sb^V-S) species (Ye et al., 2020).

Methylation and volatilization are key transformations that influence the mobility and toxicity of metal(loid)s in the environment (Caplette and Mestrot, 2021; Krishnamurthy, 1992; Pepper et al., 2015; Thayer, 2002). These transformations been investigated in biota (Dodd et al., 1996; Ji et al., 2018, 2017; Kresimon et al., 2001; Mestrot et al., 2016), soils and sediments (Caplette et al., 2021; Duester et al., 2005, 2008; Frohne et al., 2011; Grob et al., 2018; Meyer et al., 2007; Wickenheiser et al., 1998; Yang and He, 2016), oceans (Cutter et al., 2001; Cutter and Cutter, 2006, 1995), landfills (Feldmann, 2002; Feldmann and Hirner, 1995), hotsprings (Hirner et al., 1998; Planer-Friedrich and Merkel, 2006) and sewage sludge fermenters (Feldmann et al., 1994; Hirner et al., 1994; Michalke et al., 2000; Wehmeier and Feldmann, 2005). Many of these studies have focused on soluble methylated Sb species and not the volatile forms which have been detected in fewer environmental compartments (Caplette et al., 2021; Feldmann, 2002; Hirner et al., 1998; Wehmeier and Feldmann, 2005; Wickenheiser et al., 1998). The mechanism of the microbial methylation of inorganic Sb species is still unknown. Volatile Sb species may be produced as by-products of the methylation reaction (Andrewes et al., 1999; Feldmann, 2002; Meyer et al., 2008; Michalke et al., 2000; Wehmeier and Feldmann, 2005). Volatilization of Sb would increase environmental mobility and potentially cause threats to individuals living in impacted areas. For example, stibine (SbH_3) and trimethylstibine ($(CH_3)_3Sb$) are genotoxins (Andrewes et al., 2004). By using a validated and quantitative method we recently showed that flooding and manuring increased Sb volatilization in shooting range soil microcosms (Caplette et al., 2021). Our results and the study by Meyer et al. (2007) indicate that Sb volatilization may be dependent on the amount of available Sb. The lack of studies on Sb volatilization in the environment has left significant knowledge gaps about the role this mechanism plays in the global Sb biogeochemical cycle.

Organic matter, such as manure and rice straw, are commonly added as amendments in rice-agricultural practices (Kögel-Knabner et al., 2010). Organic matter amendment may influence the mobility of Sb in soils by competing with adsorption sites, forming aqueous complexes, acting as a binding agent or an electron donor in microbial respiration, and impacting the redox potential in soils (Lewińska et al., 2019; Szopka et al., 2021; Wang and Mulligan, 2006). The addition of organic matter has been reported to increase the mobility of the geochemically-similar arsenic (As) in contaminated soils (Arco-Lázaro et al., 2016; Karczewska et al., 2017; Moreno-Jiménez et al., 2013) and enhance its volatilization (Huang et al., 2012; Mestrot et al., 2009; Yan et al., 2020b). Studies on the impact of organic matter on Sb mobility are contradictory. In the presence of organic carbon, high Sb mobility has been reported in soils and waters with low Sb concentrations (Tella and Pokrovski, 2008, 2009; Verbeeck et al., 2019) along with higher Sb volatilization rates (Caplette et al., 2021), whereas other studies have suggested Sb immobilization in organic-matter rich or amended soils (Besold et al., 2019a; Grob et al., 2018; Lewińska et al., 2019; Van Vleek et al., 2011; Verbeeck et al., 2019).

Rice fields cover up to 160 million ha of the Earth's surface (Ali et al., 2020; Kögel-Knabner et al., 2010). China is one of the largest global rice producers with approximately 47 million ha of land for rice agriculture (Frolking et al., 2002; Kögel-Knabner et al., 2010). Rice fields are regularly or continuously flooded. Currently, little is known about the release of Sb in rice paddy soils and volatilization mechanisms of Sb under flooded conditions. The aim of this study is to investigate Sb release with flooding in rice-paddy soils and potential impact to the surrounding environment, and Sb volatilization mechanisms in the field and laboratory. As Sb has been shown to be released under flooded conditions due to the reductive dissolution of Fe^{III}- and Mn^{IV}-oxyhydroxides, we hypothesize that the Fe and Mn- cycles are major drivers for Sb release in rice-paddies. Additionally, the production of sulfide by sulfate reduction can sequester Sb making it less mobile. As Sb volatilization has been shown to occur under reducing conditions (Caplette et al., 2021; Feldmann, 2002; Meyer et al., 2007; Wehmeier and Feldmann, 2005) by anaerobic microorganisms (Meyer et al., 2008; Michalke et al., 2000; Wehmeier and Feldmann, 2005), rice paddy soils may represent potentially favorable sites for field-based volatile Sb measurements (Kirk, 2004; Kögel-Knabner et al., 2010). In this study, we directly investigated Sb concentrations in the surface water, porewater and soil compartments and volatilization around the Xikuangshan mining area in Hunan, China. This region has elevated soil Sb concentrations and rice agriculture (Fu et al., 2016; Liang et al., 2018; Liu et al., 2010; Okkenhaug et al., 2012; Yang and He, 2016). We also investigated the impact of flooding and cow manure amendment on Sb release and volatilization in microcosm experiments from the same rice paddy soils.

2. Materials and methods

2.1. Materials and instruments

For inductively coupled plasma mass spectrometry (ICP-MS) analysis, a 10 mg L^{-1} 29-element inorganic ICP calibration/quality control standard (Inorganic Ventures, Carl Roth, Karlsruhe, Germany) and a 1000 mg L^{-1} Sb ICP standard (Sigma-Aldrich, St. Louis, USA) were used. Supra-pur HCl (32 %) and HNO_3 (69 %) produced by the distillation (Merck Millipore Inc., Darmstadt, Germany) of p.a. grade acids in a clean-air lab were used throughout the analyses and experiments. Trace-analysis grade (≥30 %) Supelco H_2O_2 was purchased from Sigma Aldrich (Buchs, Switzerland). Ultra-pure water (>18.2 MΩ) from a Millipore Q-Gard® 2 purification

system was used. Activated coconut charcoal sorbent tubes (Anasorb CSC, 226–01, surface area of 180 m^2, SKC Inc., Eighty Four, USA) were used as Sb traps. Before use, all glassware and Teflon vials were soaked overnight in 10 % HNO_3 and rinsed with ultrapure water.

2.2. Field site information

The study area is located near Lengshuijiang, Hunan, China and is host to the largest Sb mine in the world, the Xikuangshan Mine, and two Sb smelters since 1862 (Fu et al., 2016; Liu et al., 2010; Okkenhaug et al., 2012; Wang et al., 2011) (Fig. 1a). Mineralization is hosted in Middle to Upper Devonian strata (Shetianqiao and Qiziqiao Formations), typically in silicified limestone (A'xiang and Jiantang, 2018; Liu et al., 2010; Peng et al., 2003). The major Sb ore mineral is stibnite (Sb_2S_3) (A'xiang and Jiantang, 2018; Liu et al., 2010; Peng et al., 2003). The region has a subtropical monsoon climate with up to 1400 mm annual precipitation (Liu et al., 2010).

The area surrounding the Xikuangshan Mine has been extensively studied because of the high Sb contamination and associated metal(loid)s, such as As, mercury (Hg), selenium (Se), and cadmium (Cd), in the region's soils (Bai et al., 2021; Fu et al., 2016; Okkenhaug et al., 2012; Yang and He, 2016), sediments (Liang et al., 2018; Wang et al., 2011; Yang and He, 2016) and waters (Fu et al., 2016; Liu et al., 2010; Wang et al., 2011; Zhou et al., 2017). For example, rice paddy soils have been reported to contain up to 1562 mg kg^{-1} Sb (Okkenhaug et al., 2012) and 6384 μg L^{-1} Sb in river waters (Wang et al., 2011). In the past, mine and smelter wastewaters or tailing leachates were discharged into the Qingfeng River (Fu et al., 2016; Wang et al., 2011). In the region, there is no segregation of mining and smelting activities from the residential areas. Many of the residents use lands and waters impacted by mining activities for agricultural purposes.

The field campaign took place in August 2018. Three rice paddy fields were selected based on accessibility, agricultural conditions, and the Sb concentration measured with a portable XRF (Niton XL3T pXRF Instrument) (Fig. 1a and Table S1). Site 1 is a field site with a relatively low soil Sb concentration and Sites 2 and 3 have higher Sb concentrations.

2.3. Field campaign

2.3.1. Soil sampling

In a 6 × 6-meter area, soils were sampled at the intersection of grids at 3 m intervals along the length and width of the sampling area to a 20 cm depth (n = 9 samples per site). At each sampling point, sample triplicates were collected using a soil probe, pooled, and homogenized in PE bags. The water from the paddy soil was removed before closing the sampling bags. Collected samples were stored in a cooling box, split for freeze-drying and oven drying, and frozen the day of sampling. The freeze-dried soils were stored at −20 °C until freeze-drying and the second split was oven-dried at 50 °C to a constant mass. After both drying processes, the soils were sieved (≤2 mm) and all roots and plastics were removed. The freeze-dried soils were ground (MM400 Retsch ball mill, Haan, Germany) to a fine powder and used for all chemical analyses. The oven-dried soils were used for grain size and soil pH (pH probe SenTix® 41, WTW, Weilheim, Germany).

2.3.2. Porewater and surface water sampling

Porewaters (n = 9 per site), surface waters (n = 4 per site), and irrigation waters (n = 4 total) were sampled at each field site. Porewater was sampled with each corresponding soil sample and was collected using a MOM suction cup (PVC/PE tubing, 0.15 μm pore-size, ∅ = 10 cm porous membrane) connected to a vacutainer serum tube (5 mL, BD, Allschwil, Switzerland) by a needle syringe. Paddy surface waters were collected at the corners of the sampling grid and irrigation waters were sampled at each site near the inlet. The paddy surface and irrigation waters were filtered through a 0.45 μm hydrophilic PTFE syringe filter (BGB Analytik AG, Boeckten, Switzerland). For each water sample, porewater pH and E_h (ORP probe, Lazar Research Laboratories, L.A., USA) were measured on-site immediately after sampling. Aliquots were diluted and/or acidified on-site for Sb (1:4 in 1 % HNO_3 and 0.5 % HCl), multi-elements (1:4 in 1

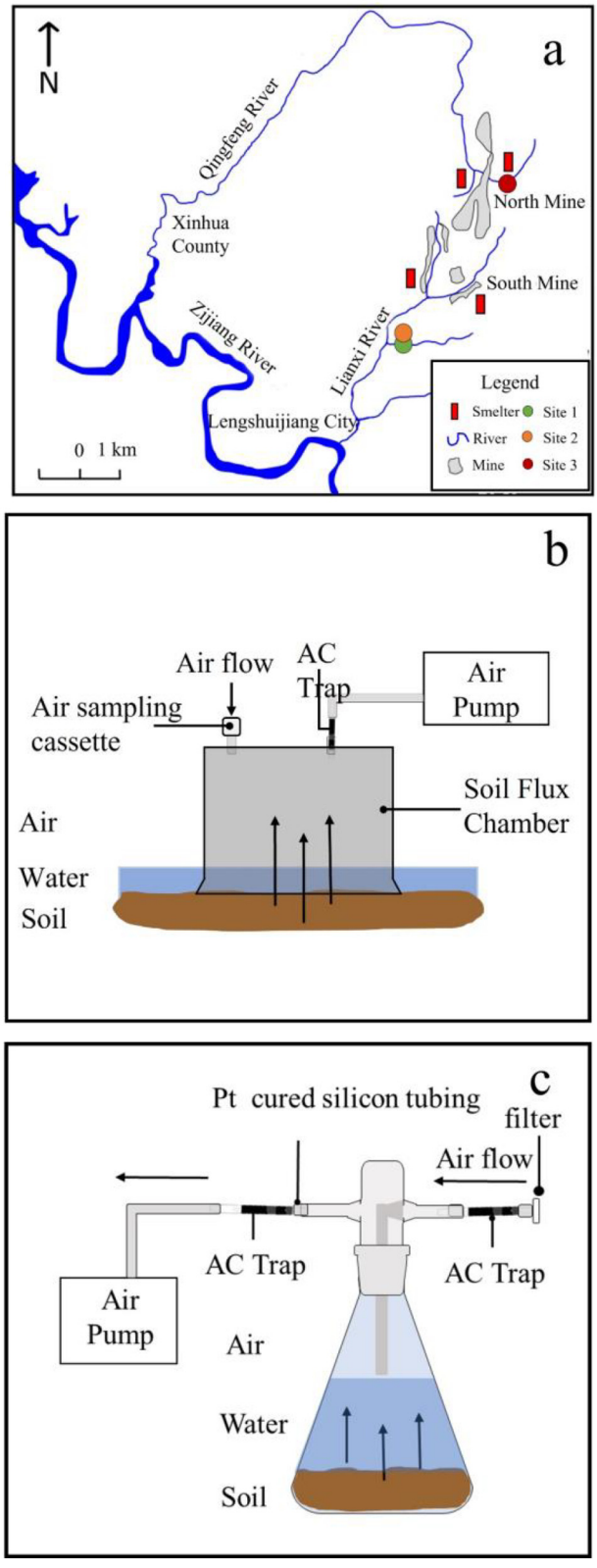

Fig. 1. a) Geographical location of the study areas field campaign region and sampling sites (map is modified (with permission) from Wang et al. (2010), b) design of the soil flux chambers for volatile Sb sampling in the field and c) experimental design for microcosm experiments (figure modified from (Caplette et al., 2021)) in the lab for soil, porewater and volatile Sb sampling.

% HNO_3), dissolved organic carbon (DOC) (1:10 in ultrapure water), and Ion Chromatography (IC) (1:5 in ultrapure water) analysis. All water samples were stored at 4 °C until further analysis.

2.3.3. Volatile Sb sampling in the field

The experimental design was modified from Mestrot et al. (2009) and Vriens et al. (2014a) for environmental Sb sampling by applying the method from Caplette et al. (2021). Six soil flux chambers were evenly distributed on the sampling grid at Site 1 and Site 3 (Fig. 1b). Each consisted of a polypropylene box with a volume of 174 L (73.1 × 53.3 × 44.5 cm) and bottom-face surface area of 0.39 m^2. The soil flux chambers were tightly placed into the soils. The outside of the soil flux chambers was covered with a commercially available opaque heat reflective cover to prevent over-heating due to greenhouse effect. Before volatile Sb sampling, the soil flux chambers were purged for 1 h (flow rate of 120 L h^{-1}). A cassette (SK-225-3050LF), with a 0.8 μm mixed cellulose ester membrane filter and 1 % (w/v) $AgNO_3$ impregnated support pad filter (Ø = 37 mm, Blanc-Labo S.A., Lonay, Switzerland), was connected to the soil flux chambers inlet to filter the in-flow air for gaseous and particulate Sb.

An activated coconut charcoal sorbent tube (Anasorb CSC, 226-01, SKC Inc., Eighty Four, USA), hereafter referred to as an Sb trap, was connected to the soil flux chamber at the outflow side on one end and to a diffusor Eheim air pump 400 modified for negative pressure (EHEIM GmbH & Co. KG, Deizisau, Germany) on the other end (Fig. 1b). Volatile Sb was sampled for 72 (Site 1) to 93 (Site 3) hours at a flow rate of 30 L h^{-1}. Ambient Sb was measured at each soil flux chamber. The ambient Sb sampling system was placed approximately 2 m above each flux chamber supported by a pole. Ambient Sb was collected by connecting the cassettes in the same configuration as the soil flux chambers to an Sb trap and was sampled for 96 (Site 1) and 93 (Site 3) hours with a flow rate of 60 L h^{-1}. Pt-cured silicone tubing ($Ø_{int}$ = 3.35 mm, VWR International, Dietikon, Switzerland) was used for all the connections.

Reported volatile Sb values are field blank subtracted. The limit of detection (LOD) for the trapping method during the field campaign corresponds to the product of 3.3 times the standard deviation (SD) of Sb concentration in the field blanks (3.3 × SD_{FB}, n = 6). The field fluxes are the quotient of the amount of Sb trapped to the area covered by the soil flux chamber and time.

2.4. Microcosm experiment

2.4.1. Experimental design

In May 2019 the three field campaigns soils were re-sampled and stored at 4 °C unit incubation. The microcosms design was similar to Caplette et al. (2021). Each microcosm consisted of an autoclaved (121 °C for 20 min), acid-washed 250 mL Erlenmeyer flask with a Drechsel head. At one end of the Drechsel's head, the in-flow air was passed through a 0.45 μm syringe filter and Sb trap (inlet trap) and the outflow air passed through an Sb trap (outlet trap) connected to a diffusor pump (600 mL min^{-1}) (Fig. 1c). All connections made with the Sb traps and microcosms were with Pt-cured silicon tubing. 150 g of each soil was added to the Erlenmeyer flasks and incubated (HPP 260, Memmert GmbH + Co. KG, Buchenbach, Germany) at 28 °C and 78 % relative humidity, the average summer temperature and humidity in the region, with two different treatments, in triplicate (n = 18), for 56 days.

In one treatment the soil was flooded (1:1 w/v soil) with N_2 purged synthetic river water, referred to as the flooded-only treatment. The recipe for the synthetic river water was calculated from reported river water values in the sampling area (Liu et al., 2010) and contained 0.70 mM Cl^-, 0.24 mM NO_3^-, 4.1 mM SO_4^{2-}, 4.1 mM Ca^{2+}, 1.7 mM Na^+, 0.97 mM Mg^{2+} and 0.19 mM K^+. For the second treatment, besides flooding the soil, 0.8 % (w/w) manure (dried cow dung, commercial available, reported Sb and metal(loid) concentrations are in Caplette et al. (2021)) was added based on standard manure application rates in rice paddies (Roy et al., 2006). The two treatments were chosen based on results from Caplette et al. (2021) indicating that Sb volatilization did not occur in non-flooded treatments.

2.4.2. Soil, porewater, and volatile Sb sampling

Soil samples were collected at the beginning and end of microcosm experiment (n = 18). Approximately 10 g of fresh soil was freeze-dried, sieved (≤2 mm), and stored for future analysis.

To collect porewater samples, a MOM suction cup (PVC/PE tubing, Ø = 5 cm porous membrane, 0.15 μm pore-size) was connected to a serum vacutainer by a needle syringe. The microcosm porewater was sampled at ten time points (1, 2, 3, 4, 7, 14, 21, 28, 42 and 56 days). At each sampling time, pH and E_h were measured using an airtight flow-through system. Aliquots for multi-element, Sb, IC, and DOC analyses were collected and stored until analysis at 4 °C. Samples were diluted for multi-element (1 % HNO_3), Sb (1 % HNO_3 + 0.5 % HCl), DOC (ultra-pure water and acidified to pH < 2), and IC (ultra-pure water). The microcosm surface waters were sampled on day 56 and filtered (≤0.45 μm), and the same aliquots as the porewaters were collected.

The Sb traps were sampled at six-time points (7, 14, 21, 28, 42, and 56 days) and stored at room temperature in the dark until digestion. At each volatile Sb sampling time, the incubators were re-watered to the starting mass with freshly prepared, N_2 purged, synthetic river water. The Sb traps were digested using an aqua regia closed vessel microwave digestion as described in Caplette et al. (2021) and the Supporting Information S2.3. The Sb trap digests were stored at 4 °C in the dark until analysis.

All reported trap values were inlet trap subtracted to account for background contamination. The LOD was calculated for each sampling time (n = 18) as 3.3 times the SD of the inlet traps (3.3 × SD_{IT}). When one of the three microcosms Sb traps was below the LOD, half the LOD was used by convention. Samples are reported as below the LOD (<LOD) when 2 or more Sb traps are below the LOD. The fluxes were calculated as the quotient of Sb trapped (ng) to the mass of soil and time.

2.5. Analysis

2.5.1. Soil digestions

Field and incubation soils were digested for Sb and multi-elements (for soil chemistry and major association of Sb in the soil) according to the protocol outlined in the Supporting Information sections S2.1 and S2.2. Sample triplicates, method blanks, and certified reference materials (CRMs, (San Joaquin soil NIST-2709a and Montana II soil 2711a, Sigma Aldrich Buchs, Switzerland)) were used. The Montana II soil CRM was acquired after the digestion of the field campaign's soils.

2.5.2. Grain size, soil pH, and CNS

For soil pH, 10 mL of 0.01 M $CaCl_2$ (1:5 m/v) was added to 2 g of the oven-dried soil. The soil was stirred, and the supernatant was measured after 2 h of equilibration. Grain size analysis was measured on the sieved, H_2O_2 pretreated soil fraction (Mastersizer 2000, Malvern PAnalytical Ltd., Malvern, United Kingdom).

For total soil carbon (C), nitrogen (N), and sulfur (S) (CNS), 10 to 40 mg of freeze-dried, ground soil was measured (Vario EL cube, Elementar Analysis system, Langenselbold, Germany) before and after loss on ignition (combusted at 550 °C for 2 h). Loss on ignition is used to estimate the soil organic C content. The organic C (C_{org}) was calculated by subtracting the C concentrations after loss on ignition. Standards of sulfanilic acid and glutamic acid, blanks, and sample triplicates were added every 16 samples for quality control.

2.5.3. Dissolved organic carbon

All porewaters, surface waters, and irrigation waters were filtered (<0.2 μm), diluted and acidified with 10 % HCl (pH < 2) for DOC analysis (Elementar Vario TOC cube, Langenselbold, Germany). Sample triplicates, blanks, and recovery checks were run every 20 samples.

2.5.4. Ion chromatography

Porewaters, irrigation waters, and surface waters from the field and microcosms were measured for dissolved anions (SO_4^{2-}, NO_3^-, PO_4^{2-}, Cl^-, NO_2^{2-}). Cations (Ca^{2+}, Na^+, K^+, NH_4^+, and Mg^{2+}) were only analyzed in the microcosm experiment. An ion chromatography Dionex Aquion™ conductivity detector system (Thermo Fisher Scientific Inc., Waltham, USA) was used for the anion (buffer: 2.7 mM Na_2CO_3 and 0.3 mM $NaHCO_3$, column: Dionex™ IonPac™ AS12A (4 × 200 mm), suppressor: Dionex™ AERS™ 500) and cation (buffer: 20 mM MSA, column: Dionex™ IonPac™ CS12A (4 × 250 mm), suppressor: Dionex™ CSRS™ 300) analyses (injection volume: 100 μL, flow rate: 1 mL min^{-1}). Each measurement included sample triplicates, recovery checks, in-house reference materials, and blanks every 20 samples.

2.5.5. Volatile antimony traps and cassettes

The digestion procedure for the Sb traps is described in Supporting Information section S2.3. Field blank traps and the inlet traps were used for background concentrations for the Sb traps collected in the field and microcosms, respectively. Method blanks and blank traps were digested with each batch. The digestion of the support pads and filters is outlined in S2.4 in the Supporting Information.

2.5.6. Elemental analysis

An Agilent 7700× series ICP-MS (Agilent Technologies, Waldbronn, Germany) was used for Sb and multi-elements analysis. Refer to Caplette et al. (2021) for further instrument and analysis details. The LOD for Sb in the soil (<0.25 mg kg^{-1}) and soil solution (<0.01 μg kg^{-1}) was calculated from method blanks.

2.5.7. Statistical treatment of data

A Students *t*-test with paired and unpaired samples ($p < 0.05$) was used to determine statistical differences. Statistical differences for temporal data were assessed using the Friedman's test followed by a Wilcoxon post-hoc test in RStudio 2021.09.01 (R Studio Team, 2021) (rstatix, ggpubr and tidyverse packages and $p < 0.05$). Pearson's r was used to assess the correlation between data. Volatile Sb outliers in the incubation study were evaluated using the interquartile range and Z-score (Reimann et al., 2008; Roessner et al., 2011). A multiple linear regression model was done by correlating data and omitting variables ($p > 0.05$) from the model.

3. Results and discussion

3.1. Field campaign

3.1.1. Environmental setting

All soils sampled were classified as Hydragric Anthrosols (Food and Agriculture Organization of the United Nations, 2006) with a silt Loam texture (USDA, 1987). The C_{org}, C/N, and pH values for the soils are reported in Supporting Information Table S2. In all three field sites the concentrations of Sb (116.0 ± 39.4 to 431.5 ± 86.5 mg kg^{-1}) and As (16.5 ± 3.1 to 58.5 ± 8.3 mg kg^{-1}, Fig. 2a and b and Table S3) in the soils are similar to most Sb-contaminated soils in the region (Bai et al., 2021; Fu et al., 2016; Okkenhaug et al., 2011; Wang et al., 2010; Wu et al., 2019) but lower than the reported value for Sb in a rice-paddy soil incubation study from the area (Okkenhaug et al., 2012). The soils at Sites 2 and 3 were the most contaminated with Sb. The soil Sb was 39 to 145 times more and As was 1.2 to 4.2 times higher than the reported background concentrations in soils (Sb: 2.98 mg kg^{-1}, As: 14 mg kg^{-1}) from the Hunan province for non-contaminated soils (Bai et al., 2021; Fu et al., 2016).

In Sites 2 and 3, the concentration of As in the sampled soils exceeds the Chinese environmental quality rice-paddy soil standards (25 mg kg^{-1}) (National Standard of the People's Republic of China, 2018). The source of As and Sb in the soils has been suggested to originate from mining and smelting activities in the region that contaminated the top-soils (Fu et al., 2016; Wang et al., 2010). Bai et al. (2021) suggested that while the Sb contamination in the region was sourced from mining and industrial practices, As contamination was geogenic based on the strong correlation with geogenically derived chromium (Cr). Our results show a relationship between soil Cr and As ($r = 0.53, p < 0.05, n = 27$) and Sb and As ($r = 0.54, p < 0.05$, n = 27) (Supporting Information section S7) indicating that the sources of As may be both anthropogenic and geogenic.

Site 1 had two irrigation water sources, one from the nearby stream (Sb: 5.0 μg L^{-1}, As: 20.2 μg L^{-1}) and one from a groundwater (Sb: 20 μg L^{-1} Sb, As: 0.4 μg L^{-1}) pumping station. At the stream source, Sb was at the cut-off value for Chinese regulatory values for surface waters but As was below it (Sb: 5 μg L^{-1}, As: 50 μg L^{-1}) (National Standard of the People's Republic of China, 2002). The groundwater source was higher for Sb but less for As than the groundwater regulations for agricultural purposes (Sb: 10 μg L^{-1}, As: 50 μg L^{-1}) (National Standard of the People's Republic of China, 2017). The irrigation waters for Sites 2 (Sb: 175.7 μg L^{-1}, As: 44.9 μg L^{-1}) and 3 (Sb: 751.2 μg L^{-1}, As: 448.4 μg L^{-1}) were highly contaminated with Sb and As when compared to the surface water quality guidelines (National Standard of the People's Republic of China, 2002).

The paddy surface waters pH ranged from 7.2 to 7.5 at the field sites. The Sb concentration in the surface waters (58.7 ± 3.8 to 495.3 ± 113.7 μg L^{-1}) was higher than the porewaters (11.7 ± 5.9 to 39.1 ± 29.0 μg L^{-1}, $p < 0.05$) (Fig. 2c and e). The surface water Sb concentration at all sites was 11.7 to 99 times higher, and the As concentration was 2.2 to 10 times higher than the Chinese drinking water guidelines (Sb: 5 μg L^{-1}, As: 10 μg L^{-1}) (Fig. 2e–f) (National Standard of the People's Republic of China, 2006). This may be due to either, the irrigation water source being contaminated with Sb (e.g., Site 3) (Hussain et al., 2021) or the diffusion of Sb from the porewater to the surface water.

The porewater pH is 6.9 and similar at all three field sites. The E_h varied between sites, at Site 1, 108.8 ± 15.4 mV, at Site 1, 127.4 ± 10.7 mV at Site 2, and at Site 3, 146.33 ± 15.9 mV ($p < 0.05$). The porewater As concentrations at Site 2 and Site 3 were similar (426.6 ± 187.3 to 368.6 ± 125.1 μg L^{-1}, $p > 0.05$) but were higher than Site 1 (190.7 ± 84.6 μg L^{-1}, $p < 0.05$) (Fig. 2d) and all sites surpassed the allowable drinking water guidelines of 10 μg L^{-1} (National Standard of the People's Republic of China, 2006). Arsenic in the waters may present a risk for rice-plant uptake and fish aquaculture in the region (Mitra et al., 2017; Panaullah et al., 2009; Talukder et al., 2012; Upadhyay et al., 2020). The porewater As correlated with Fe ($r = 0.86$ to $0.91, p < 0.05$) but not significantly with manganese (Mn) ($r < 0.65, p > 0.05$) at all field sites (Supporting Information Fig. S1a and b and section S7). Arsenic also correlated with E_h ($r = -0.79$ to -0.78, $p < 0.05$) and Co ($r = 0.77$ to $0.85, p < 0.05$) at Sites 1 and 3 and with Sb (r = 0.7 to $0.87, p < 0.05$) at Sites 1 and 2 (Supporting Information section S7). Arsenic species form inner-sphere complexes with Fe^{III}-(oxy)hydroxides (Mitsunobu et al., 2006; Ona-Nguema et al., 2005; Sherman and Randall, 2003; Yang et al., 2021), and the release of adsorbed or co-precipitated As is likely facilitated by the reductive dissolution of the Fe^{III}-phases in the soil which is a well-known process in rice paddies (Hussain et al., 2021; Liu et al., 2015; Mitsunobu et al., 2006; Takahashi et al., 2004; Yamaguchi et al., 2011; Yang et al., 2021).

3.1.2. Antimony fate in rice paddy porewaters

The Sb concentration in the porewaters was highest at Site 2 (39 ± 29.0 μg L^{-1}, $n = 9, p < 0.05$) while Site 1 (11.7 ± 5.9 μg L^{-1}, n = 9) and Site 3 (13.7 ± 3.6 μg L^{-1}, $n = 9$) had similar concentrations ($p > 0.05$) (Fig. 2c). All field sites are above the acceptable levels for Sb in drinking water (National Standard of the People's Republic of China, 2006), groundwater (National Standard of the People's Republic of China, 2017) and surface water (National Standard of the People's Republic of China, 2002).

The correlation matrices for all field sites are displayed in the Supporting Information section S7. In the Site 1 porewaters, Sb had the strongest correlations with Fe ($r = 0.76, p < 0.05$), Cu ($r = 0.69$, $p < 0.05$), As ($r = 0.87, p < 0.05$), SO_4^{2-} ($r = 0.7, p < 0.05$) and with E_h ($r = -0.77, p < 0.05$). The Site 2 porewater Sb concentrations were correlated with Co and As ($r = 0.67$ to $0.70, p < 0.05$). Although the correlation at Site 2 between Fe and Sb was not significant, Sb

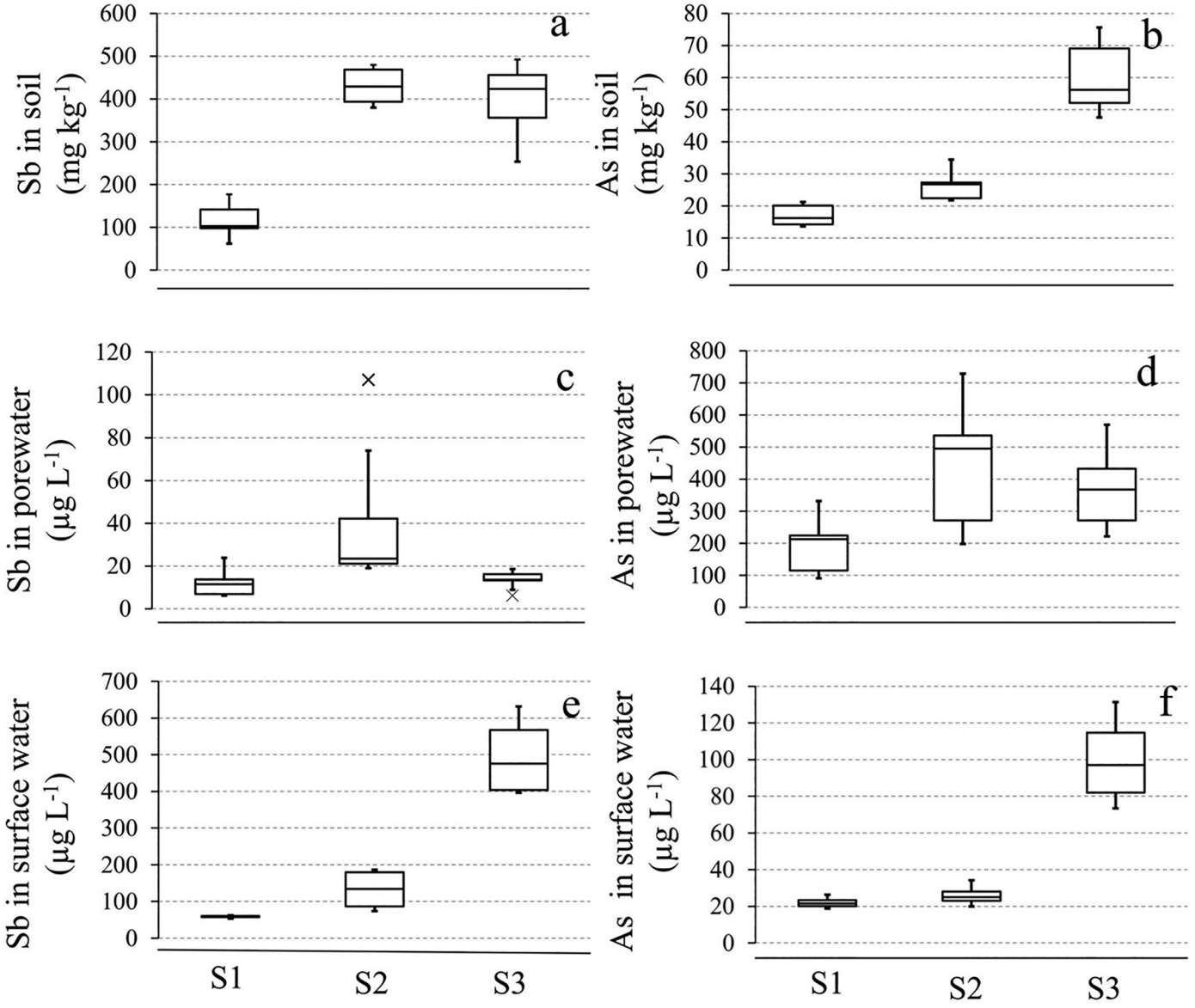

Fig. 2. Box and whisker plots for the field campaign a) Sb concentration in the soils, b) As concentration in the soils, c) total Sb concentration in porewaters, the "x" represents outlier samples, d) total As concentration in porewaters, e) total Sb concentrations in the surface waters and f) total As concentration in the surface waters. The abbreviations S1 is for Site 1, S2 is for Site 2, and S3 is for Site 3.

significantly correlated with As which correlated strongly with Fe. At Sites 1 and 2, Fe in the porewater influences porewater Sb and As concentration. The dissolution of Fe^{III}-(oxy)hydroxides likely controls the release of Sb bound to these phases at Sites 1 and 2 (Burton et al., 2019; Hockmann et al., 2014b; Mitsunobu et al., 2010; Tighe et al., 2005). Sequential extractions on the soils of the region showed that around 3 to 5 % of the Sb was associated with the reducible fractions and 60 to 80 % of the soil Sb in the soils surrounding the Xikuangshan mine area were associated with the residual fraction (Yang et al., 2015; Zhou et al., 2019). This may explain the low concentration of Sb in the porewaters. At Site 3, no significant correlations were observed with Sb. Thus, a multiple linear regression model was applied to the porewater data from Site 3 to explain the observed porewater Sb concentration (Eq. (1)).

$$Sb_{PW} = 1765.2–255.4pH - 1.14Fe_{PW} + 46Mn_{PW} + 0.02{SO_4}^{2-}{}_{PW} \quad (1)$$

where Sb_{PW} is the concentration of Sb in the porewater in µg L^{-1}, pH is the porewater pH, Fe_{PW}, Mn_{PW}, and ${SO_4}^{2-}{}_{PW}$ are the concentrations of Fe, Mn, and SO_4^{2-} in the porewater in mg L^{-1}, respectively. The model has an $R^2 = 0.91$ ($p < 0.05$) and could predict 86.8 to 108.6 % of the Sb concentrations from Site 3. A major driver for Sb mobility in soils and sediments is pH, where Sb^V, as an anion, has a more pH dependent mobility than Sb^{III} (Mitsunobu et al., 2006; Wilson et al., 2010). The porewaters at Site 3 contained less ($p < 0.05$) Fe, Mn, and Sb than Site 2 although the soils had similar Sb concentrations. Sb forms inner-sphere complexes with Fe- and Mn-(oxy)hydroxides, and Sb release into porewaters has been shown to be associated with the reductive dissolution of Mn minerals in soils (Belzile et al., 2001; Hockmann et al., 2014b; Wilson et al., 2010). The primary Sb mineral in the region is stibnite the oxidation of sulfide minerals could produce SO_4^{2-} (Biver and Shotyk, 2012; Xiang et al., 2022).

3.1.3. Volatile Sb emissions from rice paddy soils

Volatile Sb has been measured in the environment (Caplette et al., 2021; Feldmann, 2002; Hirner et al., 1998; Michalke et al., 2000; Wickenheiser et al., 1998) but never quantitatively from soils. We

report here the very first quantitative measurements of volatile Sb from soils in the environment.

Antimony was only detected on the inlet cassette filters and not on the support pads (below instrument LOD, 0.006 μg L^{-1}) indicating that the filters successfully removed particulate Sb from the in-flow air. For ambient Sb sampling, the cassette filters, representing particulate matter, contained 241.1 ± 22.5 ng m^{-3} Sb at Site 1 and 600.6 ± 240.3 ng m^{-3} at Site 3 (Supporting Information Fig. S4). At Site 1, the soil flux chambers in-flow filters had 269.8 ± 24.7 ng m^{-3} Sb and Site 3 had 416.1 ± 245.7 ng m^{-3} Sb.

Volatile Sb on the ambient traps was above the LOD (2.01 ng Sb or LOD_{flux} = 4.9 mg ha^{-1} y^{-1}) in four of six Sb traps at Site 1 and only two of six traps at Site 3. The ambient volatile Sb measured at Site 1 and Site 3 ranged from <LOD – 3.3 ng m^{-3} (n = 12). Volatile Sb was detected from the soil flux chambers Sites 1 and 3. Volatile Sb, was above the LOD in three of the six Sb traps at Site 1 (5.8 ± 1.7 ng Sb) and five of the six Sb traps at Site 3 (90.1 ± 66.5 ng Sb) (Fig. 3). The volatile Sb detected on the outlet traps was similar to the ambient traps at Site 1 ($p > 0.05$) but higher at Site 3 ($p < 0.05$).

An average flux of 18.1 ± 5.2 mg ha^{-1} y^{-1} for Site 1 and 217.9 ± 160.7 mg ha^{-1} y^{-1} for Site 3, up to 18 times higher at Site 3 than Site 1 ($p < 0.05$). Volatile Sb emissions at Site 3 were higher than the ambient Sb sampled, suggesting that Sb volatilization is from the rice paddies. There was no significant difference in porewater Sb concentration between Sites 1 and 3 and no observed correlation between porewater Sb and volatile Sb production ($r < 0.45$, $p > 0.05$, n = 7). Contrary to As volatilization in rice paddies (Mestrot et al., 2011), our results suggest that the porewater Sb may not be driving Sb volatilization in the rice paddies. The small sample size (n = 12, but only 7 were greater than the LOD) did not allow for a representative correlation analysis with the measured volatile Sb.

3.2. Microcosm study

Our previous work indicated that flooded conditions were favorable for Sb volatilization in shooting range soils (Caplette et al., 2021). As agricultural practices, such as organic matter amendments, can enhance As release and volatilization in soils (Edvantoro et al., 2004; Mestrot et al., 2009; Moreno-Jiménez et al., 2013; Wang and Mulligan, 2006; Yan et al., 2020b) and Sb volatilization (Caplette et al., 2021) a treatment with manure was included in the microcosm study.

The incubated soils have similar Sb and As concentrations as the field campaign soils (Table S4). The soils were incubated at 28 °C for 56 days. Soil porewaters and Sb traps were collected at daily to weekly intervals to evaluate the release of Sb and the production of volatile Sb throughout the experiment.

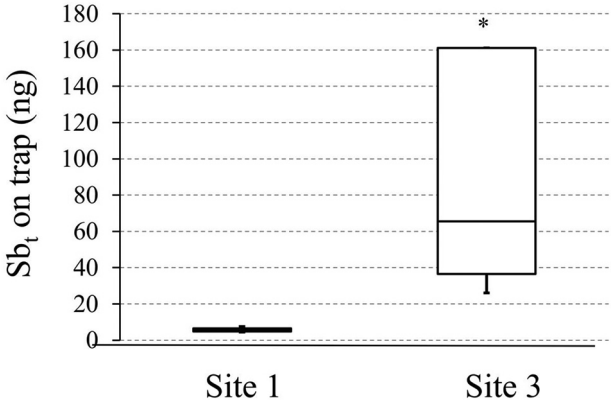

Fig. 3. Box and whisker plot for volatile Sb collected on the outlet trap of the closed flow-through box system in the field. Asterisk (*) indicates that the sample was >0 for a one-sided t-test ($p < 0.05$).

3.2.1. Porewater pH and E_h

In both treatments, the porewater pH slightly increased and stabilized after a week of incubation, while the E_h decreased following a constant raise after a week or two of incubation (Fig. S5). The manure-amended microcosms had a lower pH than the flooded-only treatments ($p < 0.05$) (Fig. S5a, b, and c). This may be explained by the production of organic acids by fermentation and CO_2 from anaerobic respiration, and subsequent production of carbonic acid (Boyd, 1995; Kögel-Knabner et al., 2010; Reddy and DeLaune, 2008). Manuring the soils lowered the E_h (Fig. S5d, e, and f) and increased Fe- and Mn- release in the porewaters, an indication of dissimilatory Fe- and Mn- reduction, which is a proton-consuming reaction (Kögel-Knabner et al., 2010; Rinklebe et al., 2017).

3.2.2. Influence of manure addition on Sb release

The total Sb released throughout the experiment (56 days) was similar for the manured (291.9 to 2189.3 μg·d L^{-1}) and the flooded-only treatments (303.7 to 2066.3 μg·d L^{-1}) ($p > 0.05$) (Fig. a, c, and e). The addition of amendments, such as phosphate, have been shown to enhance Sb release into porewaters, likely caused by competition for sorption sites, in microcosm experiments from soils in the same region (Okkenhaug et al., 2012). Previous studies with shooting range soils (Grob et al., 2018) and mine dump soils (Lewińska et al., 2018) showed that the addition of organic matter and waterlogging also enhanced Sb release. This may be caused by competitive sorption of organic molecules with Sb onto reactive minerals surfaces, complexation of Sb species with labile organic molecules, or enhanced anaerobic respiration and, in turn, more Fe and Mn release into the porewaters. The maximum Sb released in the studies by Grob et al. (2018) and Lewińska et al. (2018) is higher than our study. This may be due to the larger proportion of organic matter (2 to 5 % (w/w) vs. 0.8 % (w/w) here) added although the soils contained less Sb than our study. We aimed in this study to follow realistic manuring application rates for rice paddies.

3.2.3. Sb release with sulfate

All microcosms had at least one release phase. The first phase of Sb release was triggered by flooding followed by a rapid decrease (Fig. 4a, c, and e). In the manured and flooded-only treatments for Site 2 and the flooded-only treatment at Site 3, there was a second phase of Sb release (Fig. 4a, c, and e).

In all treatments, Sb release was highest during the first day, decaying within four days, consistent with previous studies (Grob et al., 2018; Tandy et al., 2018). The concentration of Sb in the porewaters for the entire experiment at Sites 2 and 3 exceeded the Chinese guidelines for Sb in drinking waters and groundwaters for agricultural use regardless of treatment (National Standard of the People's Republic of China, 2017, 2006). For the Site 1 soils, porewater Sb only exceeded regulation values during the first release phase of the experiment (National Standard of the People's Republic of China, 2017, 2006).

The highest measured Sb concentration (84 μg L^{-1}) was in the manured Site 3 soil. For the duration of the experiment, the highly contaminated soils (Sites 2 and 3) released more Sb in the porewater compared to the low-contaminated soil at Site 1 ($p < 0.05$). With flooding, Sb was released into the porewaters, the manured treatments released a maximum of 49.5 ± 10.1 to 64.4 ± 26.6 μg L^{-1} and the flooded-only treatments were similar ($p > 0.05$), releasing 37.5 ± 11.9 to 75.5 ± 4.5 μg L^{-1}. Rice paddy soil incubations, using soil from the same region but with 3 to 12.6 times higher Sb concentration, released up to 2000 μg L^{-1} Sb in the porewaters (Okkenhaug et al., 2012). For the manured soils during the initial release phase porewater Sb concentrations were higher in our study than in a shooting range soil (2.4–110 mg kg^{-1} Sb) in Norway (Okkenhaug et al., 2018) and incubated Swiss shooting range soil (21 mg kg^{-1} Sb) (Hockmann et al., 2014a).

With flooding, all microcosms initially had a high Sb release and rapidly declined within four days. Rapid release of Sb with flooding has also been observed in shooting range (Grob et al., 2018; Hockmann et al., 2014a; Lewińska et al., 2019; Wan et al., 2013a) and mine dump soils (Lewińska

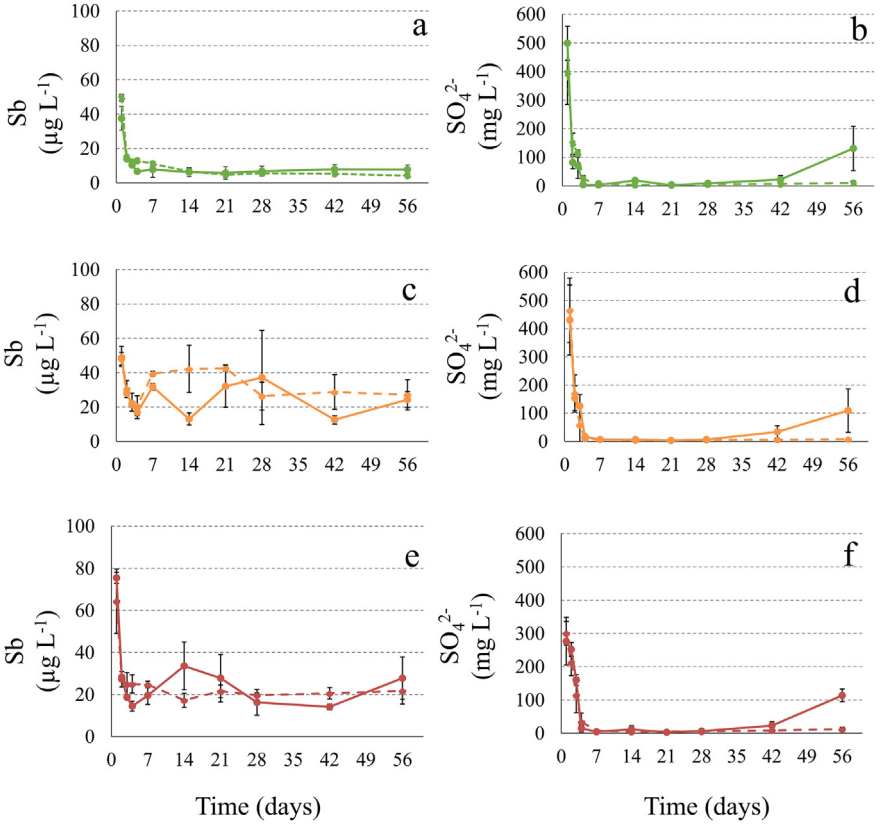

Fig. 4. Temporal porewater results for flooded-only (solid line) and flooded manured (dashed line) microcosms for a) Sb in site 1, b) SO_4^{2-} in Site 1, c) Sb in Site 2, d) SO_4^{2-} in site 2, e) Sb in site 3, and f) SO_4^{2-} in site 3. Results presented as the average of triplicate microcosms and the standard deviation. The lines between sampling points are interpolations for better readability.

et al., 2018) and may be caused by the release of weakly bound Sb and/or dissolution of soluble salts. A sudden high release of Sb with flooding may have environmental implications with rice agriculture as rice fields are typically flooded at the beginning of the growing season. When flooded, Sb may be temporarily mobilized in the rice fields.

There was a negative correlation between Sb and Fe concentrations during the initial release-immobilization phase ($r = -0.58$ to -0.88, $p < 0.05$, $n = 12$ per site), indicating that the onset of Fe reduction was not the initial driver of Sb into the porewaters when flooded (Figs. 4 and 5). In all microcosms, the Sb concentration rapidly declined by the fourth day and was similar to the porewater SO_4^{2-} decline (Figs. 4b, d, and f). Porewater Sb and SO_4^{2-} correlated ($r = 0.71$ to 0.91, $p < 0.05$, $n = 30$ per treatment) in both treatments with the Site 1 soil (Fig. 4a) and the manured treatment with the Site 3 soil (Fig. 4e). Antimony and SO_4^{2-} correlated ($r = 0.7$ to 0.94, $p < 0.05$, $n = 12$ per treatment) during the mobilization – immobilization phase (four days) for both treatments with the Site 2 soil (Fig. 4c) and the flooded-only treatment with Site 3 soil (Fig. 4e). Antimony and SO_4^{2-} may be liberated from the solid-phase by the desorption of weakly-bound species (Grob et al., 2018; Hockmann et al., 2014a; Wan et al., 2013b) and/or dissolution of soluble salts (Doner and Lynn, 1989) caused by the initial disequilibrium with flooding.

The observed loss of porewater Sb and SO_4^{2-} may be explained by two possible mechanisms: 1) by the rapid re-absorption or structural incorporation of Sb onto/into Fe^{III}-(oxy)hydroxides, or 2) by dissimilatory sulfate reduction and immobilization of Sb by sulfides or complexation with organic thiol groups.

The decrease in porewater Sb concentration could be from re-adsorption onto the solid phase by the fourth day of incubation as suggested by Grob et al., 2018 and Hockmann et al., 2014b. The reduction of Sb^V to Sb^{III} and its stronger sorption onto Fe^{III}-(oxy)hydroxides (Hockmann et al., 2015, 2014a; Lewińska et al., 2019) or the structural incorporation of Sb into recrystallized Fe^{III}-(oxy)hydroxides facilitated by production of Fe^{II} have been reported to immobilize Sb under reducing conditions (Burton et al., 2019; Hockmann et al., 2021; Karimian et al., 2019a; Mitsunobu et al., 2010). In the study by Okkenhaug et al. (2012) the porewater speciation of Sb was dominated by Sb^V.

Flooding may induce SO_4^{2-} reduction producing reduced sulfur species (Kirk, 2004; Reddy and DeLaune, 2008; Rinklebe et al., 2017). Sulfate reduction in our system was not confirmed with E_h measurements (≤ -100 mV) (Kirk, 2004; Reddy and DeLaune, 2008; Rinklebe et al., 2017) but it should be mentioned that our redox measurements are bulk measurements of the whole system and that more reduced hotspots may exist. Decreasing molar ratios of $[SO_4^{2-}]$:$[Cl^-]$ indicate that SO_4^{2-} reduction may be occurring (Supporting Information Fig. S6a, d, and g) (Gfeller et al., 2021; Karisiddaiah et al., 2006; Matson and Brinson, 1985; Sass et al., 2003). In a contaminated floodplain soil, Weber et al. (2009a, 2009b) showed SO_4^{2-} consumption within 4 to 10 days after flooding a contaminated floodplain soil, occurring simultaneously with Fe- and Mn- reduction with similar E_h values as this study. Similar results were observed in flooded rice-paddy soils showing rapid Sb mobility with the onset of flooding and rapid reduction corresponding to the reduction of SO_4^{2-} in the porewaters (Xia et al., 2022).

Reduced mobility of Sb caused by complexation to organic sulfur or by the formation of authigenic Sb-sulfides (e.g., amorphous SbS_3) has been reported in anoxic sediments (Chen et al., 2003; Polack et al., 2009), wetland sediments (Arsic et al., 2018; Bennett et al., 2017), and rice paddies (Xia et al., 2022). However, it has been also shown that Sb release in oxic-anoxic sediment incubations from the same area was not coupled to the S-cycle (Ye et al., 2020). The authors instead suggested redox transformations were controlling Sb solubility. Okkenhaug et al. (2012) reported Sb-solubility was likely controlled by Ca-romeite ($Ca_{1+x}Sb_2O_6(OH_{2-2x})$) group minerals in paddy soils from the same region. Lewińska et al. (2018) speculated that a rapid reduction in Sb solubility in high-contaminated mine dump soils was facilitated by Sb saturation and the

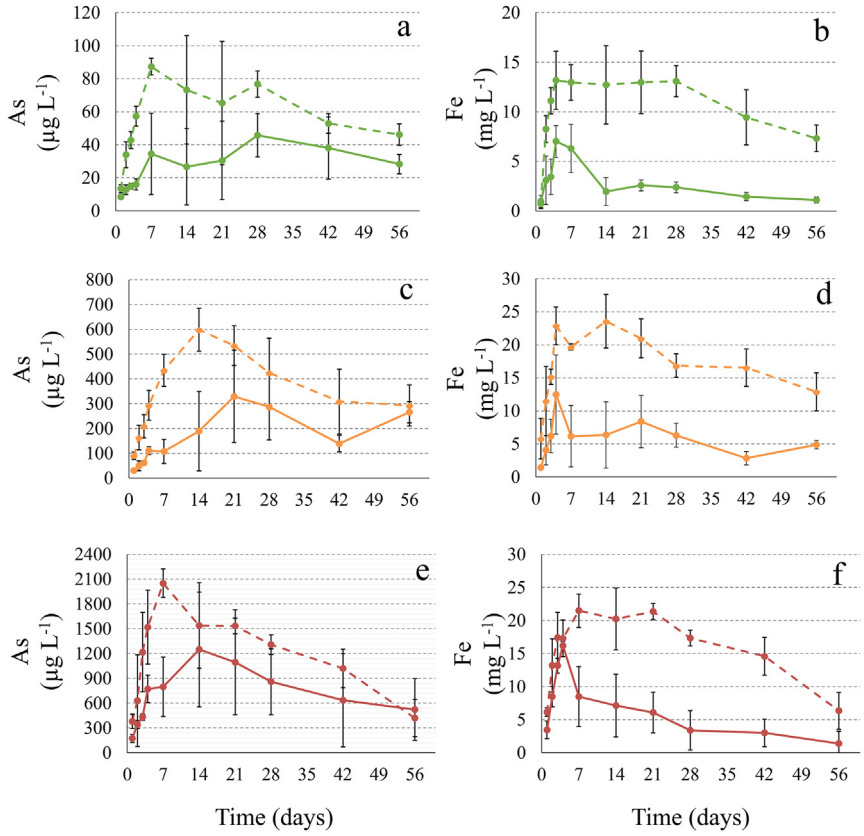

Fig. 5. Temporal results for flooded-only (solid line) and flooded manured (dashed line) microcosms for a) As in site 1, b) Fe in site 1, c) As in Site 2, d) Fe in site 2, e) As in site 3, and f) Fe in site 3. Results presented as the average of triplicate microcosms and the standard deviation. The y axis scale differs for each figure and the lines between sampling points are interpolations for better readability.

formation of authigenic calcium antimonate and romeite phases. In our study, we did not observe any significant relationship between porewater Sb and Ca^{2+} ($r = -0.3$–0.27, $p > 0.05$, Supporting Information section S7). Based on our results, we speculate that the rapid release of Sb in our system was controlled by the initial desorption of Sb from the solid phase and rapid Sb immobilization was caused by Sb sequestration with sulfide phases.

3.2.4. Sb release in porewaters by reductive iron dissolution

A rise in Sb concentration in the flooded-only Site 2 microcosms occurred on day seven (Fig. 4c). A temporary increase in porewater Sb concentration was detected in only the high-Sb contaminated soils of Sites 2 and 3. This temporary increase in porewater Sb was associated with Fe and As in the flooded-only treatments at Site 2 (14 to 56 days, $r = 0.56$ for Fe and $r = 0.77$ for As, $p < 0.05$, $n = 15$) and Site 3 (7 to 28 days, $r = 0.6$ for Fe and $r = 0.9$ for As, $p < 0.05$, $n = 12$) soils (Figs. 4a, c and e and 5). Up to 39.7 ± 19.7 µg L^{-1} Sb was released from the flooded-only Site 3 soil. For the manured treatment of Site 2 soil, where up to 42.7 ± 3.3 µg L^{-1} Sb was released between days 7 to 28, it was not significantly correlated with Fe ($r = 0.45, p > 0.05\ n = 18$) but correlated with As ($r = 0.66$, $p < 0.05, n = 18$) which also correlated strongly with Fe ($r = 0.81, p < 0.05$, $n = 18$). At the end of the experiment, a relative increase in porewater Sb was observed in the flooded-only Site 2 and 3 soils (Fig. 4c and e). This was not significant ($p > 0.05$, $n = 6$ per site) when compared to earlier sampling days (i.e., days 28 and 42).

Waterlogging induces the reductive dissolution of redox-sensitive host phases which can enhance Sb mobility in the environment. But, Fe^{II} in soil and sediment porewaters can also induce recrystallization of Fe^{III}-phases that can structurally incorporate Sb^{V} and immobilize it (Hockmann et al., 2021, 2020; Karimian et al., 2019a; Mitsunobu et al., 2010). The release of Sb caused by the reductive dissolution of Fe^{III}-(oxy) hydroxides have been well documented in waterlogged shooting range soils (Grob et al., 2018; Hockmann, 2014; Hockmann et al., 2014b; Tandy et al., 2018) and rice-paddy soils (Xia et al., 2022).

3.2.5. Sb in surface waters

The surface waters were sampled on the last day of the microcosm experiment. The surface waters had 40.7 ± 27.7 to 484.0 ± 102.9 µg L^{-1} Sb, consistent with the surface waters in the field campaign and much higher than the porewater Sb concentrations. The surface waters are approximately 4–48 times higher than the regulations for Chinese drinking and agricultural waters (National Standard of the People's Republic of China, 2017, 2006). The synthetic river water used for the experiment did not contain any detectable Sb (below instrument LOD, <0.006 µg L^{-1} Sb). Diffusion of Sb from the porewaters to the surface waters was the likely source of Sb in the surface waters. This data may suggest that Sb in the porewaters may also diffuse to the surface waters in the field sites and could therefore be a source of Sb in the surface waters, as well as the contaminated irrigation waters.

3.2.6. As release

Manuring the soils released more As in all microcosms ($p < 0.05$) (Fig. 5a, c, and e). Manure application has been shown to increase As solubility by up to 19 % in rice paddy soils (Tang et al., 2021; Yang et al., 2021). The highest release of As into the porewaters, 2505.8 ± 171.8 µg L^{-1}, was observed from the manured treatment at Site 3 which has the highest soil As concentration. In both treatments, except for the Site 3 manured treatment, As correlated with porewater Mn during the first 4 days of the experiments ($p > 0.05$) and Fe, in stages, throughout the experiment ($r = 0.45$ to $0.9, p < 0.05$). Our results are consistent with typical As behavior in flooded soils, and with Fe^{III}-(oxy)hydroxides controlled solubility in soils (Lewińska et al., 2019; Mitsunobu et al., 2006; Okkenhaug et al., 2012; Takahashi

et al., 2004; Yang et al., 2021). The reductive dissolution of Fe^{III}-phases in the soil release As into the surrounding porewaters and enhances the mobility of As in the environment (Takahashi et al., 2004). The high As concentration in porewaters indicates a high potential for rice-plant uptake. One of the major exposure pathways of As to humans is through the ingestion of rice (Chung et al., 2014; Guo et al., 2021; Lee et al., 2008; Mondal and Polya, 2008; Panaullah et al., 2009; Vahter and Concha, 2001). Arsenic release was higher than Sb in our experiment porewaters, this indicates that As may present a higher risk to the rice plants in the Xikuangshan mining area than Sb.

3.2.7. Volatile Sb production in microcosms

One sample, the Site 3 flooded only soil on day 42, was 3 times higher than the interquartile range and had a Z-score of 2.5. As the datum was skewed from the mean, it was omitted from the statistical treatment of the data as it likely represents contamination. The LOD for each sampling time is in the Supporting Information Table S5. The LOD_{flux} is 0.67 ng kg^{-1} d^{-1} for the entire experiment.

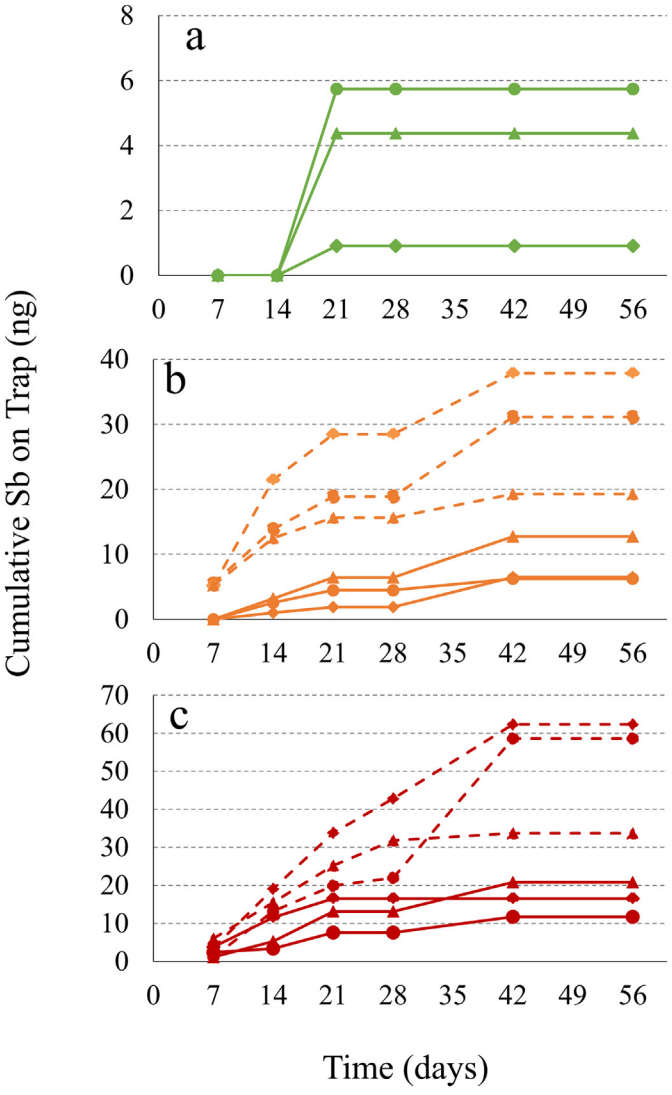

Fig. 6. Production of cumulative volatile Sb throughout the experiment for flooded-only (solid line) and flooded manured (dashed line) microcosms for a) site 1, b) site 2, and c) site 3. All microcosms outlet traps are inlet trap subtracted to correct for background contamination. Samples below experimental LOD, when 2 of 3 microcosms are larger than the LOD, are replaced with 0.5 × LOD. The symbols for the microcosm replicates are: circle (replicate 1), diamond (replicate 2), and triangle (replicate 3).

Significantly more volatile Sb was produced from the Site 2 and 3 soils than from the Site 1 soils (Table S5, Fig. 6). In most cases, the Site 1 samples were below the LOD. The manure-treated soils produced significantly more ($p < 0.05$) volatile Sb with 1278.1 ± 409.1 to 2237.5 ± 679.7 ng kg^{-1} y^{-1} than the flooded-only treatments with 159.6 ± 108.4 to 709.9 ± 197.0 ng kg^{-1} y^{-1} (Table S5). Organic matter likely stimulates microbial activity enhancing volatilization as shown before for both Sb and As (Caplette et al., 2021; Edvantoro et al., 2004; Mestrot et al., 2011). Higher amounts of manure resulted in higher Sb volatilization even in soils with lower soil Sb concentrations (Fig. 6) (Caplette et al., 2021). The highest cumulative flux (2237.5 ± 679.7 ng kg^{-1} y^{-1}) of volatile Sb was in the manured Site 3 soil. The peak volatile Sb production was observed on the fourteenth day of the experiment, equating to 776.1 to 4299.2 ng kg^{-1} y^{-1} Sb. It is possible that the availability of Sb in our system is lower than in the shooting range soils (Caplette et al., 2021) due to, for example, soil mineralogy, and may be another possible reason for the lower volatilization rates.

On the last day of the experiment (day 56), all microcosms were below the experimental LOD, showing that volatilization had effectively stopped (Table S5, Fig. 6). Although more volatile Sb was detected in the higher Sb-containing soils in this study, higher Sb volatilization rates were reported from soils with lower Sb concentrations (Caplette et al., 2021; Meyer et al., 2007). This demonstrates that the drivers of Sb volatilization are still largely unknown but substrate Sb concentration may not the main driver for Sb volatilization. Other factors may also be important drivers for Sb volatilization such as the organic matter content, bioavailable Sb, temperature, and microbial composition of the soil. High Sb and As levels may hinder Sb volatilizing microorganisms, as previously shown for As volatilization (Frankenberger, 1998).

It is inferred that Sb is likely hosted in refractory phases due to the minimal solubility observed in our study and extraction results from paddy soils in the region (Okkenhaug et al., 2011; Zhou et al., 2019). The proportion of the soil Sb volatilized was 0.00002 to 0.000085 %, lower than previously reported in shooting range soils (0.0004 to 0.002 %) (Caplette et al., 2021), microorganisms (0.001 to 2.3 %) (Jenkins et al., 1998; Smith et al., 2002; Wehmeier and Feldmann, 2005), and alluvial soils (2.8 %) (Meyer et al., 2007).

A correlation analysis between total released porewater Sb (area under the curve approach), surface water Sb and the cumulative volatile Sb showed that volatile Sb is not correlated with porewater Sb ($r = -0.1$ to 0.4, $p > 0.05$, $n = 9$ per treatment) but with the surface water Sb concentration for both treatments ($r = 0.85$ to 0.89, $p < 0.05$, $n = 5$ and 7 depending on treatment) (Fig. 7). Although the majority of the microorganisms shown to methylate and volatilize Sb are anaerobes (Meyer et al., 2008; Michalke et al., 2000; Wehmeier et al., 2004; Wehmeier and Feldmann, 2005), it has also been observed in aerobic microorganisms (Andrewes et al., 2001, 2000, 1999; Smith et al., 2002). Sb volatilization in the investigated soils may be occurring in the surface waters and not in the porewaters as previously hypothesized for shooting range soils (Caplette et al., 2021) and arsines (Mestrot et al., 2011). Vriens et al. (2014b) showed that volatile As species, which are structurally similar to Sb species, correlated linearly and parabolically with surface waters in an Ombrotrophic peat bog.

3.3. Global production of volatile Sb

Our results indicate that volatile Sb is produced in the aerobic surface waters from flooded environments. These results have implications from an environmental perspective as wetlands account for 5 to 10 % of the terrestrial environment (Kingsford et al., 2016) and rice-paddy soils comprise 160 million ha globally (Kögel-Knabner et al., 2010). With the assumption that all rice paddies contain Sb and have constant emissions, we upscaled our results by calculating Sb emissions from rice paddies based on the global rice field coverage. The microcosm experiments produced 24 to 1625 mg ha^{-1} y^{-1} of volatile Sb equating to 4 to 260 t y^{-1} (Table 1) globally. The emissions from the field campaign are <LOD to 62 t y^{-1} (Table 1). The Sb emissions in our study, which are based on rice paddies, could account up to 13.6 % of the global anthropogenic Sb emissions. These results

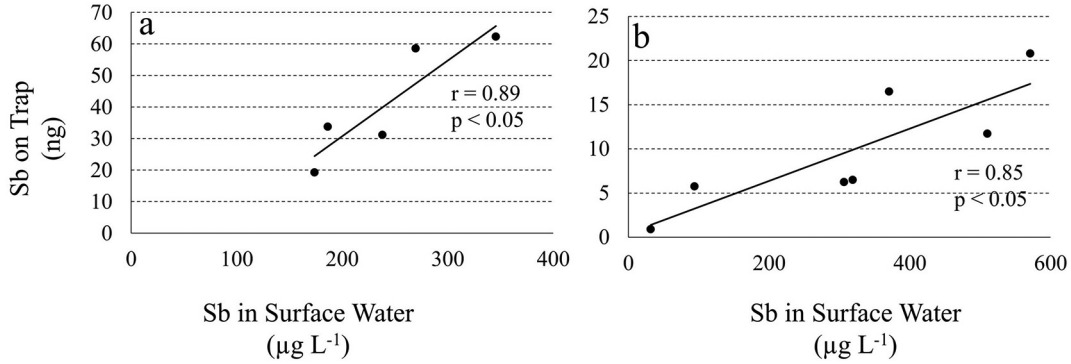

Fig. 7. Correlation of Sb produced during the microcosm experiment with surface water in a) flooded manured treatments and b) flooded-only treatments. The lines represent the line of best fit using the least squares method.

are estimations and likely do not represent realistic Sb emissions from rice paddies which have variable Sb concentrations. Many factors will also likely influence volatilization rates throughout the year (e.g., seasonal flooding or consistent flooding and temperature). Additionally, the environmental impacts of gaseous Sb emissions (e.g., rice paddies) compared to particulate emissions (e.g., anthropogenic sources) should be taken into consideration.

The anthropogenic Sb emissions in 2010 were estimated at 1905 t (Tian et al., 2014) (Table S6). The major anthropogenic source of Sb to the atmosphere was 803 t from fuel combustion, non-ferrous metal production emitted 320 t, waste incineration emitted 455 t, brake wear emitted 318 t, and pig iron and steel production emitted the least at 9 t (Tian et al., 2014) (Table S6). The predicted amount for rice paddy fields Sb volatilization based on our results is less than the global emissions from most anthropogenic sources except for pig iron and steel production and represents a significant portion of the anthropogenic emissions. Our preliminary estimates show that Sb emissions from rice paddy soils may account for <LOD – 9.8 % of the estimated natural global Sb emissions (2651 t, (Nriagu, 1989)), sole study to have investigated global natural Sb emission sources (Table S6). Our results are higher than reported values for biogenic marine and continental volatile emissions but are in the same order of magnitude.

As high organic matter content is typical of wetlands and the addition of organic matter influences the amount of volatile Sb produced, these sites represent favorable environments for Sb volatilization (Caplette et al., 2021; Wickenheiser et al., 1998; Yan et al., 2020a). The amount of soluble Sb in surface waters may be an important driver for Sb volatilization, and soils that are periodically or consistently flooded with contaminated waters or contaminated soils releasing Sb with waterlogging, such as floodplain soils may be of interest. If volatilization is occurring in the aerobic surface waters, studying oceanic environments may be of interest as methylated Sb species have been detected in the Atlantic and Pacific Oceans (Cutter et al., 2001; Cutter and Cutter, 2006, 1995). The ocean is an important source of structurally similar arsines to the atmosphere (Savage et al., 2018, 2019).

4. Conclusion

In rice-paddy soils surrounding the Xikuangshan Mine, porewater Sb concentrations were generally low indicating minimal potential for soil-plant transfer. The volatilization of Sb from soils was quantified for the first time in the field and more volatile Sb was produced from a high Sb-contaminated paddy field. Our work shows that volatile Sb is produced in the environment and may play a significant role in Sb mobility and cycling in the environment. Further work investigating volatile Sb production with mesocosms would be beneficial to better understand the process in the environment.

Microcosm treatment type (with or without manure) and soil Sb concentration did not influence Sb release into the porewaters. Using a manure amendment did not influence the release of Sb to the porewaters, indicating minimal risk of manuring to the surrounding environment. During the flooding stage of rice-agriculture Sb is released into the porewaters posing risk with flooding. The Sb concentration quickly decreases in the porewater corresponding with SO_4^{2-}, suggesting immobilization caused by SO_4^{2-} reduction. A secondary release of Sb associated with Fe reduction and As release was observed in some microcosms indicating the role of Fe and the potential for more Sb mobilization during the rice growing season which may pose a threat to the aquaculture and rice plants in the paddies. Further studies should investigate the temporal solid-phase partitioning of Sb in these systems to give better insight into the role of mineral and phase transformations coupling with Sb mobility.

In the microcosm experiments, volatile Sb correlated with Sb concentration in the surface waters indicating that volatilization could be occurring

Table 1
Sb fluxes from the field campaign and microcosm soils, global emission estimates (t y^{-1}) and the proportion of the emissions with respect to the total anthropogenic emissions in Tian et al. (2014), natural emissions in Nriagu (1989) and the global total emissions. The acronym F is for the flooded only treatments and FM is for the flooded and manured treatments. The global fluxes were calculated from the global area of rice paddies.

	Fluxes mg ha^{-1} y^{-1}	Global emissions t y^{-1}	Proportion of global emissions (%)		
			Anthropogenic	Natural	Total
		Field campaign			
Site 1	<LOD - 24	<LOD - 4	<LOD - 0.2	<LOD - 0.1	<LOD - 0.05
Site 3	63–390	10–62	0.5–3.3	0.4–2.3	0.2–1.4
Microcosms					
Site 1_F	24–150	4–24	0.2–1.3	0.1–0.9	0.1–0.5
Site 1_FM					
Site 2_F	162–332	26–53	1.4–2.8	1.0–2.0	0.6–1.2
Site 2_FM	502–987	80–158	4.2–8.3	3.0–6.0	1.8–3.5
Site 3_F	306–542	49–87	2.6–4.6	1.8–3.3	1.1–1.9
Site 3_FM	875–1625	140–260	7.3–13.6	5.3–9.8	3.1–5.7

in the aerobic surface waters. By manuring the soils more volatile Sb was produced. Although only 0.000085 % of the soil Sb was volatilized, Sb volatilization could account for a large proportion of Sb to the atmosphere, up to 13.6 % of the anthropogenic emissions, and in turn influence the Sb cycle on a larger scale. However, these estimations represent an extrapolation from our currently small dataset. Thus, we emphasize the importance of further work on the factors that influence Sb volatilization in the field and in microcosm experiments, the role of Sb speciation on volatilization, and inputs to the atmosphere.

Funding sources

This work was supported by the Swiss National Science Foundation (SNSF, grant number 163661) to A. Mestrot.

CRediT authorship contribution statement

Jaime N. Caplette: Conceptualization, Formal Analysis, Methodology, Writing – original draft, Writing – review & editing, Investigation, Visualization, Project Administration. Lorenz Gfeller: Investigation, Resources, Writing – review & editing. Da Lei: Investigation, Resources, Writing – review & editing. Jie Liao: Investigation, Resources, Writing – review & editing. Jicheng Xia: Investigation, Resources, Writing – review & editing. Hua Zhang: Resources, Writing – review & editing. Xinbin Feng: Resources, Writing – review & editing, Funding acquisition, Project Administration. Adrien Mestrot: Supervision, Conceptualization, Writing – review & editing, Funding acquisition, Project Administration.

Declaration of competing interest

The authors declare that they have no known competing financial interests or personal relationships that could have appeared to influence the work reported in this paper.

Acknowledgements

J. Caplette would like to thank Dr. Fisher, A. Weber, and M. Bishoff for their help with analyzing the DOC and IC samples, P. Neuhaus for help with ICP-MS measurements, L. Stanisic for help with ICP-MS measurements, sample preparation, digestions, and sampling, S. Pfister and A. Weber for their assistance with sample collection, experimental set-up, digestions and multiple analyses, H. Guan for her assistance with document translation and A. Foetisch and Dr. K. Viacava for their help editing the manuscript.

Appendix A. Supporting information

Supporting information to this article can be found online at https://doi.org/10.1016/j.scitotenv.2022.156631.

References

A'xiang, H., Jiantang, P., 2018. Fluid inclusions and ore precipitation mechanism in the giant Xikuangshan mesothermal antimony deposit, South China: conventional and infrared microthermometric constraints. Ore Geology Reviews 95, 49–64. https://doi.org/10.1016/j.oregeorev.2018.02.005.

Ali, W., Mao, K., Zhang, H., Junaid, M., Xu, N., Rasool, A., Feng, X., Yang, Z., 2020. Comprehensive review of the basic chemical behaviours, sources, processes, and endpoints of trace element contamination in paddy soil-rice systems in rice-growing countries. J. Hazard. Mater. 397, 122720. https://doi.org/10.1016/j.jhazmat.2020.122720.

Andrewes, P., Cullen, W.R., Polishchuk, E., 1999b. Confirmation of the aerobic production of trimethylstibine by scopulariopsis brevicaulis. Appl. Organometal. Chem. 13, 659–664. https://doi.org/10.1002/(SICI)1099-0739(199909)13:9<659::AID-AOC895>3.0.CO;2-J.

Andrewes, P., Cullen, W.R., Polishchuk, E., 2000. Arsenic and antimony biomethylation by scopulariopsis brevicaulis : interaction of arsenic and antimony compounds. Environ. Sci. Technol. 34, 2249–2253. https://doi.org/10.1021/es991269p.

Andrewes, P., Cullen, W.R., Polishchuk, E., Reimer, K.J., 2001. Antimony biomethylation by the wood rotting fungusPhaeolus schweinitzii. Appl. Organometal. Chem. 15, 473–480. https://doi.org/10.1002/aoc.131.

Andrewes, P., Kitchin, K.T., Wallace, K., 2004. Plasmid DNA damage caused by stibine and trimethylstibine. Toxicol. Appl. Pharmacol. 194, 41–48. https://doi.org/10.1016/j.taap.2003.08.012.

Arco-Lázaro, E., Agudo, I., Clemente, R., Bernal, M.P., 2016. Arsenic(V) adsorption-desorption in agricultural and mine soils: effects of organic matter addition and phosphate competition. Environ. Pollut. 216, 71–79. https://doi.org/10.1016/j.envpol.2016.05.054.

Arsic, M., Teasdale, P.R., Welsh, D.T., Johnston, S.G., Burton, E.D., Hockmann, K., Bennett, W.W., 2018. Diffusive gradients in thin films reveals differences in antimony and arsenic mobility in a contaminated wetland sediment during an oxic-anoxic transition. Environ. Sci. Technol. 52, 1118–1127. https://doi.org/10.1021/acs.est.7b03882.

Bai, J., Zhang, W., Liu, W., Xiang, G., Zheng, Y., Zhang, X., Yang, Z., Sushkova, S., Minkina, T., Duan, R., 2021. Implications of soil potentially toxic elements contamination, distribution and health risk at Hunan's xikuangshan mine. Processes 9, 1532. https://doi.org/10.3390/pr9091532.

Belzile, N., Chen, Y.-W., Wang, Z., 2001b. Oxidation of antimony (III) by amorphous iron and manganese oxyhydroxides. Chem. Geol. 174, 379–387. https://doi.org/10.1016/S0009-2541(00)00287-4.

Belzile, N., Chen, Y.-W., Filella, M., 2011. Human exposure to antimony: I. Sources and intake. Crit. Rev. Environ. Sci. Technol. 41, 1309–1373. https://doi.org/10.1080/10643381003608227.

Bennett, W.W., Hockmann, K., Johnston, S.G., Burton, E.D., 2017. Synchrotron X-ray absorption spectroscopy reveals antimony sequestration by reduced sulfur in a freshwater wetland sediment. Environ. Chem. 14, 345. https://doi.org/10.1071/EN16198.

Besold, J., Eberle, A., Noël, V., Kujala, K., Kumar, N., Scheinost, A.C., Pacheco, J.L., Fendorf, S., Planer-Friedrich, B., 2019a. Antimonite binding to natural organic matter: spectroscopic evidence from a mine water impacted peatland. Environ. Sci. Technol. 53, 10792–10802. https://doi.org/10.1021/acs.est.9b03924.

Besold, J., Kumar, N., Scheinost, A.C., Lezama Pacheco, J., Fendorf, S., Planer-Friedrich, B., 2019b. Antimonite complexation with thiol and Carboxyl/Phenol groups of peat organic matter. Environ. Sci. Technol. 53, 5005–5015. https://doi.org/10.1021/acs.est.9b00495.

Biver, M., Shotyk, W., 2012. Stibnite (Sb2S3) oxidative dissolution kinetics from pH 1 to 11. Geochim. Cosmochim. Acta 79, 127–139. https://doi.org/10.1016/j.gca.2011.11.033.

Boyd, C.E., 1995. Soil organic matter, anaerobic respiration, and oxidation—reduction. Bottom Soils, Sediment, and Pond Aquaculture. Springer US, Boston, MA, pp. 194–218 https://doi.org/10.1007/978-1-4615-1785-6_6.

Burton, E.D., Johnston, S.G., Kocar, B.D., 2014. Arsenic mobility during flooding of contaminated soil: the effect of microbial sulfate reduction. Environ. Sci. Technol. 48, 13660–13667. https://doi.org/10.1021/es503963k.

Burton, E.D., Hockmann, K., Karimian, N., Johnston, S.G., 2019. Antimony mobility in reducing environments: the effect of microbial iron(III)-reduction and associated secondary mineralization. Geochim. Cosmochim. Acta 245, 278–289. https://doi.org/10.1016/j.gca.2018.11.005.

Caplette, J.N., Mestrot, A., 2021. Biomethylation and biovolatilization of antimony. Antimony. De Gruyter, pp. 251–274.

Caplette, J.N., Grob, M., Mestrot, A., 2021. Validation and deployment of a quantitative trapping method to measure volatile antimony emissions. Environ. Pollut. 289, 117831. https://doi.org/10.1016/j.envpol.2021.117831.

CEC, 1998. Council Directive 98/83/EC of 3 November 1998 on the Quality of Water Intended for Human Consumption.

Chen, Y.-W., Deng, T.-L., Filella, M., Belzile, N., 2003. Distribution and early diagenesis of antimony species in sediments and porewaters of Freshwater Lakes. Environ. Sci. Technol. 37, 1163–1168. https://doi.org/10.1021/es025931k.

Chung, J.-Y., Yu, S.-D., Hong, Y.-S., 2014. Environmental source of arsenic exposure. J. Prev. Med. Public Health 47, 253–257. https://doi.org/10.3961/jpmph.14.036.

Cutter, G.A., Cutter, L.S., 1995. Behavior of dissolved antimony, arsenic, and selenium in the Atlantic Ocean. Mar. Chem. 49, 295–306. https://doi.org/10.1016/0304-4203(95)00019-N.

Cutter, G.A., Cutter, L.S., 2006. Biogeochemistry of arsenic and antimony in the North Pacific Ocean: arsenic and antimony cycles. Geochem. Geophys. Geosyst. 7, 1–12. https://doi.org/10.1029/2005GC001159.

Cutter, G.A., Cutter, L.S., Featherstone, A.M., Lohrenz, S.E., 2001. Antimony and arsenic biogeochemistry in the western Atlantic Ocean. Deep-Sea Res. II Top. Stud. Oceanogr. 48, 2895–2915. https://doi.org/10.1016/S0967-0645(01)00023-6.

Dodd, M., Pergantis, S.A., Cullen, W.R., Li, H., Eigendorf, G.K., Reimer, K.J., 1996. Antimony speciation in freshwater plant extracts by using hydride generation–gas chromatography–mass spectrometry. Analyst 121, 223–228. https://doi.org/10.1039/AN9962100223.

Doner, H.E., Lynn, W.C., 1989. Carbonate, halide, sulfate, and sulfide minerals. In: Dixon, J.B., Weed, S.B. (Eds.), SSSA Book Series. Soil Science Society of America, Madison, WI, USA, pp. 279–330 https://doi.org/10.2136/sssabookser1.2ed.c6.

Duester, L., Diaz-Bone, R.A., Kösters, J., Hirner, A.V., 2005. Methylated arsenic, antimony and tin species in soils. J. Environ. Monit. 7, 1186. https://doi.org/10.1039/b508206d.

Duester, L., Vink, J.P.M., Hirner, A.V., 2008. Methylantimony and -arsenic species in sediment pore water tested with the sediment or Fauna incubation experiment. Environ. Sci. Technol. 42, 5866–5871. https://doi.org/10.1021/es800272h.

Edvantoro, B.B., Naidu, R., Megharaj, M., Merrington, G., Singleton, I., 2004. Microbial formation of volatile arsenic in cattle dip site soils contaminated with arsenic and DDT. Appl. Soil Ecol. 25, 207–217. https://doi.org/10.1016/j.apsoil.2003.09.006.

Feldmann, J., 2002. Volatilization of metals from a landfill site: generation and immobilization of volatile species of tin, antimony, bismuth, mercury, arsenic, and tellurium on a municipal waste deposit in Delta, British Columbia. In: Cai, Y., Braids, O.C. (Eds.), Biogeochemistry of Environmentally Important Trace Elements, ACS Symposium Series. American Chemical Society, Washington, DC, pp. 128–140. https://doi.org/10.1021/bk-2003-0835.ch010.

Feldmann, J., Hirner, A.V., 1995. Occurrence of volatile metal and metalloid species in landfill and sewage gases. Int. J. Environ. Anal. Chem. 60, 339–359. https://doi.org/10.1080/03067319508042888.

Feldmann, J., Grumping, R., Hirner, A.V., 1994. Determination of volatile metal and metalloid compounds in gases from domestic waste deposits with GC/ICP-MS. Fresenius J. Anal. Chem. 350, 228–234. https://doi.org/10.1007/BF00322474.

Filella, M., Belzile, N., Chen, Y.-W., 2002. Antimony in the environment: a review focused on natural waters I. Occurrence. Earth-Science Reviews 57, 125–176. https://doi.org/10.1016/S0012-8252(01)00070-8.

Food and Agriculture Organization of the United Nations (Ed.), 2006. World reference base for soil resources, 2006: a framework for international classification, correlation, and communication, 2006, ed. ed World soil resources reports. Food and Agriculture Organization of the United Nations, Rome (Ed.).

Frankenberger, W.T., 1998. Short communication: effects of trace elements on arsenic volatilization. Soil Biol. Biochem. 30, 6. https://doi.org/10.1016/S0038-0717(97)00102-8.

Frohne, T., Rinklebe, J., Diaz-Bone, R.A., Du Laing, G., 2011. Controlled variation of redox conditions in a floodplain soil: impact on metal mobilization and biomethylation of arsenic and antimony. Geoderma 160, 414–424. https://doi.org/10.1016/j.geoderma.2010.10.012.

Frolking, S., Qiu, J., Boles, S., Xiao, X., Liu, J., Zhuang, Y., Li, C., Qin, X., 2002. Combining remote sensing and ground census data to develop new maps of the distribution of rice agriculture in China: paddy rice cropland maps for China. Glob. Biogeochem. Cycl. 16. https://doi.org/10.1029/2001GB001425 38-1-38–10.

Fu, Z., Wu, F., Mo, C., Deng, Q., Meng, W., Giesy, J.P., 2016. Comparison of arsenic and antimony biogeochemical behavior in water, soil and tailings from xikuangshan, China. Sci. Total Environ. 539, 97–104. https://doi.org/10.1016/j.scitotenv.2015.08.146.

Gfeller, L., Weber, A., Worms, I., Slaveykova, V.I., Mestrot, A., 2021. Mercury mobility, colloid formation and methylation in a polluted fluvisol as affected by manure application and flooding–draining cycle. Biogeosciences 18, 3445–3465. https://doi.org/10.5194/bg-18-3445-2021.

Grob, M., Wilcke, W., Mestrot, A., 2018. Release and biomethylation of antimony in shooting range soils upon flooding. Soil Syst. 2, 34. https://doi.org/10.3390/soilsystems2020034.

Guo, X., Wu, Z., He, M., Meng, X., Jin, X., Qiu, N., Zhang, J., 2014. Adsorption of antimony onto iron oxyhydroxides: adsorption behavior and surface structure. J. Hazard. Mater. 276, 339–345. https://doi.org/10.1016/j.jhazmat.2014.05.025.

Guo, W., Zhang, Z., Wang, H., Qin, H., Fu, Z., 2021. Exposure characteristics of antimony and coexisting arsenic from multi-path exposure in typical antimony mine area. J. Environ. Manag. 289, 112493. https://doi.org/10.1016/j.jenvman.2021.112493.

Hirner, A.V., Feldmann, J., Goguel, R., Rapsomanikis, S., Fischer, R., Andreae, M.O., 1994. Volatile metal and metalloid species in gases from municipal waste deposits. Appl. Organomet. Chem. 8, 65–69. https://doi.org/10.1002/aoc.590080111.

Hirner, A.V., Feldmann, J., Krupp, E., Grümping, R., Goguel, R., Cullen, W.R., 1998. Metal (loid)organic compounds in geothermal gases and waters. Org. Geochem. 29, 1765–1778. https://doi.org/10.1016/S0146-6380(98)00153-3.

Hockmann, K., Lenz, M., Tandy, S., Nachtegaal, M., Janousch, M., Schulin, R., 2014a. Release of antimony from contaminated soil induced by redox changes. J. Hazard. Mater. 275, 215–221. https://doi.org/10.1016/j.jhazmat.2014.04.065.

Hockmann, K., Tandy, S., Lenz, M., Schulin, R., 2014b. Antimony leaching from contaminated soil under manganese- and iron-reducing conditions: column experiments. Environ. Chem. 11, 624. https://doi.org/10.1071/EN14123.

Hockmann, K., Tandy, S., Lenz, M., Reiser, R., Conesa, H.M., Keller, M., Studer, B., Schulin, R., 2015. Antimony retention and release from drained and waterlogged shooting range soil under field conditions. Chemosphere 134, 536–543. https://doi.org/10.1016/j.chemosphere.2014.12.020.

Hockmann, K., Planer-Friedrich, B., Johnston, S.G., Peiffer, S., Burton, E.D., 2020. Antimony mobility in sulfidic systems: coupling with sulfide-induced iron oxide transformations. Geochim. Cosmochim. Acta 282, 276–296. https://doi.org/10.1016/j.gca.2020.05.024.

Hockmann, K., Karimian, N., Schlagenhauff, S., Planer-Friedrich, B., Burton, E.D., 2021. Impact of Antimony(V) on Iron(II)-catalyzed ferrihydrite transformation pathways: a novel mineral switch for feroxyhyte formation. Environ. Sci. Technol. 55, 4954–4963. https://doi.org/10.1021/acs.est.0c08660.

Huang, H., Jia, Y., Sun, G.-X., Zhu, Y.-G., 2012. Arsenic speciation and volatilization from flooded paddy soils amended with different organic matters. Environ. Sci. Technol. 46, 2163–2168. https://doi.org/10.1021/es203635s.

Hussain, M.M., Bibi, I., Niazi, N.K., Shahid, M., Iqbal, J., Shakoor, M.B., Ahmad, A., Shah, N.S., Bhattacharya, P., Mao, K., Bundschuh, J., Ok, Y.S., Zhang, H., 2021. Arsenic biogeochemical cycling in paddy soil-rice system: interaction with various factors, amendments and mineral nutrients. Sci. Total Environ. 773, 145040. https://doi.org/10.1016/j.scitotenv.2021.145040.

Jenkins, R.O., Craig, P.J., Miller, D.P., 1998. Antimony Biomethylation by Mixed Cultures of Micro-organisms Under Anaerobic Conditions. 12, pp. 449–455. https://doi.org/10.1002/(SICI)1099-0739(199806)12:6<449::AID-AOC719>3.0.CO;2-4.

Ji, Y., Sarret, G., Schulin, R., Tandy, S., 2017. Fate and chemical speciation of antimony (Sb) during uptake, translocation and storage by rye grass using XANES spectroscopy. Environ. Pollut. 231, 1322–1329. https://doi.org/10.1016/j.envpol.2017.08.105.

Ji, Y., Mestrot, A., Schulin, R., Tandy, S., 2018. Uptake and transformation of methylated and inorganic antimony in plants. Front. Plant Sci. 9, 140. https://doi.org/10.3389/fpls.2018.00140.

Karczewska, A., Gałka, B., Dradrach, A., Lewińska, K., Mołczan, M., Cuske, M., Gersztyn, L., Litak, K., 2017. Solubility of arsenic and its uptake by ryegrass from polluted soils amended with organic matter. J. Geochem. Explor. 182, 193–200. https://doi.org/10.1016/j.gexplo.2016.11.020.

Karimian, N., Burton, E.D., Johnston, S.G., 2019a. Antimony speciation and mobility during Fe(II)-induced transformation of humic acid-antimony(V)-iron(III) coprecipitates. Environ. Pollut. 254, 113112. https://doi.org/10.1016/j.envpol.2019.113112.

Karimian, N., Burton, E.D., Johnston, S.G., Hockmann, K., Choppala, G., 2019b. Humic acid impacts antimony partitioning and speciation during iron(II)-induced ferrihydrite transformation. Sci. Total Environ. 683, 399–410. https://doi.org/10.1016/j.scitotenv.2019.05.305.

Karisiddaiah, S.M., Borole, D.V., Ramalingeswara Rao, B., Paropkari, A.L., Joao, H.M., Muralidhar, K., Sarkar, G.P., Biswas, G., Kumar, N., 2006. Studies on the pore water sulphate, chloride and sedimentary methane to understand the sulphate reduction process in eastern Arabian Sea. Curr. Sci. 91, 8.

Kingsford, R.T., Basset, A., Jackson, L., 2016. Wetlands: conservation's poor cousins: wetland conservation. Aquatic Conserv: Mar. Freshw. Ecosyst. 26, 892–916. https://doi.org/10.1002/aqc.2709.

Kirk, G., 2004. The Biogeochemistry of Submerged Soils. 1st ed. Wiley https://doi.org/10.1002/047086303X.

Kögel-Knabner, I., Amelung, W., Cao, Z., Fiedler, S., Frenzel, P., Jahn, R., Kalbitz, K., Kölbl, A., Schloter, M., 2010. Biogeochemistry of paddy soils. Geoderma 157, 1–14. https://doi.org/10.1016/j.geoderma.2010.03.009.

Kresimon, J., Grüter, U., Hirner, A., 2001. HG/LT–GC/ICP–MS coupling for identification of metal(loid) species in human urine after fish consumption. Fresenius J. Anal. Chem. 371, 586–590. https://doi.org/10.1007/s002160101087.

Krishnamurthy, S., 1992. Biomethylation and environmental transport of metals. J. Chem. Educ. 69, 347. https://doi.org/10.1021/ed069p347.

Lee, J.-S., Lee, S.-W., Chon, H.-T., Kim, K.-W., 2008. Evaluation of human exposure to arsenic due to rice ingestion in the vicinity of abandoned myungbong Au–Ag mine site, Korea. J. Geochem. Explor. 96, 231–235. https://doi.org/10.1016/j.gexplo.2007.04.009.

Leuz, A.-K., Mönch, H., Johnson, C.A., 2006. Sorption of Sb(III) and Sb(V) to goethite: influence on Sb(III) oxidation and mobilization †. Environ. Sci. Technol. 40, 7277–7282. https://doi.org/10.1021/es061284b.

Lewińska, K., Karczewska, A., Siepak, M., Gałka, B., 2018. The release of antimony from mine dump soils in the presence and absence of Forest litter. IJERPH 15, 2631. https://doi.org/10.3390/ijerph15122631.

Lewińska, K., Karczewska, A., Siepak, M., Szopka, K., Gałka, B., Iqbal, M., 2019. Effects of waterlogging on the solubility of antimony and arsenic in variously treated shooting range soils. Appl. Geochem. 105, 7–16. https://doi.org/10.1016/j.apgeochem.2019.04.005.

Liamleam, W., Annachhatre, A.P., 2007. Electron donors for biological sulfate reduction. Biotechnol. Adv. 25, 452–463. https://doi.org/10.1016/j.biotechadv.2007.05.002.

Liang, Z., Hua, Z., Jia, P., Liu, J., Luo, Z., Chen, W., Kuang, J., Liao, B., Shu, W., Li, J., 2018. Strong associations between biogeochemical factors and sb species in sediments of the World's largest sb mine (Xikuangshan) in China. J. Geophys. Res. Biogeosci. 123, 1548–1556. https://doi.org/10.1029/2018JG004481.

Liu, F., Le, X.C., McKnight-Whitford, A., Xia, Y., Wu, F., Elswick, E., Johnson, C.C., Zhu, C., 2010. Antimony speciation and contamination of waters in the Xikuangshan antimony mining and smelting area, China. Environ. Geochem. Health 32, 401–413. https://doi.org/10.1007/s10653-010-9284-z.

Liu, C., Yu, H.-Y., Liu, Chengshuai, Li, F., Xu, X., Wang, Q., 2015. Arsenic availability in rice from a mining area: is amorphous iron oxide-bound arsenic a source or sink? Environ. Pollut. 199, 95–101. https://doi.org/10.1016/j.envpol.2015.01.025.

Matson, E.A., Brinson, M.M., 1985. Sulfate enrichments in estuarine waters of North Carolina. Estuaries 8, 279. https://doi.org/10.2307/1351488.

Mestrot, A., Uroic, M.K., Plantevin, T., Islam, Md.R., Krupp, E.M., Feldmann, J., Meharg, A.A., 2009. Quantitative and qualitative trapping of arsines deployed to assess loss of volatile arsenic from Paddy soil. Environ. Sci. Technol. 43, 8270–8275. https://doi.org/10.1021/es9018755.

Mestrot, A., Feldmann, J., Krupp, E.M., Hossain, M.S., Roman-Ross, G., Meharg, A.A., 2011. Field fluxes and speciation of arsines emanating from soils. Environ. Sci. Technol. 45, 1798–1804. https://doi.org/10.1021/es103463d.

Mestrot, A., Ji, Y., Tandy, S., Wilcke, W., 2016. A novel method to determine trimethylantimony concentrations in plant tissue. Environ. Chem. 13, 919. https://doi.org/10.1071/EN16018.

Meyer, J., Schmidt, A., Michalke, K., Hensel, R., 2007. Volatilisation of metals and metalloids by the microbial population of an alluvial soil. Syst. Appl. Microbiol. 30, 229–238. https://doi.org/10.1016/j.syapm.2006.05.001.

Meyer, J., Michalke, K., Kouril, T., Hensel, R., 2008. Volatilisation of metals and metalloids: an inherent feature of methanoarchaea? Syst. Appl. Microbiol. 31, 81–87. https://doi.org/10.1016/j.syapm.2008.02.001.

Michalke, K., Wickenheiser, E.B., Mehring, M., Hirner, A.V., Hensel, R., 2000. Production of volatile derivatives of Metal(loid)s by microflora involved in anaerobic digestion of sewage sludge. Appl. Environ. Microbiol. 66, 2791–2796. https://doi.org/10.1128/AEM.66.7.2791-2796.2000.

Mitra, A., Chatterjee, S., Moogouei, R., Gupta, D., 2017. Arsenic accumulation in rice and probable mitigation approaches: a review. Agronomy 7, 67. https://doi.org/10.3390/agronomy7040067.

Mitsunobu, S., Harada, T., Takahashi, Y., 2006. Comparison of antimony behavior with that of arsenic under various soil redox conditions. †Environ. Sci. Technol. 40, 7270–7276. https://doi.org/10.1021/es060694x.

Mitsunobu, S., Takahashi, Y., Terada, Y., Sakata, M., 2010. Antimony(V) incorporation into synthetic ferrihydrite, goethite, and natural iron oxyhydroxides. Environ. Sci. Technol. 44, 3712–3718. https://doi.org/10.1021/es903901e.

Mondal, D., Polya, D.A., 2008. Rice is a major exposure route for arsenic in chakdaha block, Nadia district, West Bengal, India: a probabilistic risk assessment. Appl. Geochem. 23, 2987–2998. https://doi.org/10.1016/j.apgeochem.2008.06.025.

Moreno-Jiménez, E., Clemente, R., Mestrot, A., Meharg, A.A., 2013. Arsenic and selenium mobilisation from organic matter treated mine spoil with and without inorganic fertilisation. Environ. Pollut. 173, 238–244. https://doi.org/10.1016/j.envpol.2012.10.017.

Muller, T., Craw, D., McQuillan, A.J., 2015. Arsenate and antimonate adsorption competition on 6-line ferrihydrite monitored by infrared spectroscopy. Appl. Geochem. 61, 224–232. https://doi.org/10.1016/j.apgeochem.2015.06.005.

National Standard of the Peoples Republic of China, 2002. GB 3838-2002 Environmental Quality Standards for Surface Water.

National Standard of the Peoples Republic of China, 2006. GB 5749-2006 Standards for Drinking Water Quality.
National Standard of the Peoples Republic of China, 2017. GB/T 14848-2017 Standard for Groundwater Quality.
National Standard of the Peoples Republic of China, 2018. GB 1518-2018 Soil Environmental Quality Risk Management Standards for Soil Contamination of Agricultural Lands.
Nriagu, J.O., 1989. A global assessment of natural sources of atmospheric trace metals. Nature 338, 47–49. https://doi.org/10.1038/338047a0.
Nriagu, J., Bhattacharya, P., Mukherjee, A., Bundschuh, J., Zevenhoven, R., Loeppert, R., 2007. Arsenic in soil and groundwater: an overview. Trace Metals in the Environment. Elsevier, pp. 3–60 https://doi.org/10.1016/S0927-5215(06)09001-1.
Okkenhaug, G., Zhu, Y.-G., Luo, L., Lei, M., Li, X., Mulder, J., 2011. Distribution, speciation and availability of antimony (Sb) in soils and terrestrial plants from an active Sb mining area. Environ. Pollut. 159, 2427–2434. https://doi.org/10.1016/j.envpol.2011.06.028.
Okkenhaug, G., Zhu, Y.-G., He, J., Li, X., Luo, L., Mulder, J., 2012. Antimony (Sb) and arsenic (As) in sb mining impacted Paddy soil from xikuangshan, China: differences in mechanisms controlling soil sequestration and uptake in Rice. Environ. Sci. Technol. 46, 3155–3162. https://doi.org/10.1021/es2022472.
Okkenhaug, G., Smebye, A.B., Pabst, T., Amundsen, C.E., Sævarsson, H., Breedveld, G.D., 2018. Shooting range contamination: mobility and transport of lead (Pb), copper (Cu) and antimony (Sb) in contaminated peatland. J. Soils Sediments 18, 3310–3323. https://doi.org/10.1007/s11368-017-1739-8.
Ona-Nguema, G., Morin, G., Juillot, F., Calas, G., Brown, G.E., 2005. EXAFS analysis of arsenite adsorption onto two-line ferrihydrite, hematite, goethite, and lepidocrocite. Environ. Sci. Technol. 39, 9147–9155. https://doi.org/10.1021/es050889p.
Panaullah, G.M., Alam, T., Hossain, M.B., Loeppert, R.H., Lauren, J.G., Meisner, C.A., Ahmed, Z.U., Duxbury, J.M., 2009. Arsenic toxicity to rice (Oryza sativa L.) in Bangladesh. Plant Soil 317, 31–39. https://doi.org/10.1007/s11104-008-9786-y.
Peng, J.-T., Hu, R.-Z., Burnard, P.G., 2003. Samarium–neodymium isotope systematics of hydrothermal calcites from the xikuangshan antimony deposit (Hunan, China): the potential of calcite as a geochronometer. Chem. Geol. 200, 129–136. https://doi.org/10.1016/S0009-2541(03)00187-6.
Pepper, I.L., Gerba, C.P., Gentry, T.J. (Eds.), 2015. Environmental Microbiology, Thirdedition Elsevier/AP, Academic Press is an imprint of Elsevier, Amsterdam.
Planer-Friedrich, B., Merkel, B.J., 2006. Volatile metals and metalloids in hydrothermal gases. Environ. Sci. Technol. 40, 3181–3187. https://doi.org/10.1021/es051476r.
Polack, R., Chen, Y.-W., Belzile, N., 2009. Behaviour of Sb(V) in the presence of dissolved sulfide under controlled anoxic aqueous conditions. Chem. Geol. 262, 179–185. https://doi.org/10.1016/j.chemgeo.2009.01.008.
R Studio Team, 2021. RStudio: Integrated Development Environment for R. RStudio, PBC, Boston, MA.
Reddy, R.K., DeLaune, R.D., 2008. Biogeochemistry of Wetlands: Science and Applications. 1st ed. CRC Press.
Reimann, C., Filzmoser, P., Garrett, R.G., Dutter, R., 2008. Statistical Data Analysis Explained. John Wiley & Sons Ltd, Chichester, UK https://doi.org/10.1002/9780470987605.
Trace elements in waterlogged soils and sediments. In: Rinklebe, J., Knox, A.S., Paller, M.H. (Eds.), Advances in Trace Elements in the Environment. CRC Press, Taylor & Francis Group, Boca Raton.
Roessner, U., Nahid, A., Chapman, B., Hunter, A., Bellgard, M., 2011. Metabolomics – the combination of analytical biochemistry, biology, and informatics. Comprehensive Biotechnology. Elsevier, pp. 447–459 https://doi.org/10.1016/B978-0-08-088504-9.00052-0.
Roy, R.N., Finck, A., Blair, G.J., Tandon, H.L.S., 2006. Plant Nutrition for Food Security: A Guide for Integrated Nutrient Management. FAO fertilizer and plant nutrition bulletin, Rome.
Sass, H., Rütters, H., Schledjewski, R., 2003. The Influence of Seasonal Changes on the Microbial Communities in the Wadden Sea. Berichte - Forschungszentrum Terramare. 4.
Savage, L., Carey, M., Williams, P.N., Meharg, A.A., 2018. Biovolatilization of arsenic as arsines from seawater. Environ. Sci. Technol. 52, 3968–3974. https://doi.org/10.1021/acs.est.7b06456.
Savage, L., Carey, M., Williams, P.N., Meharg, A.A., 2019. Maritime deposition of organic and inorganic arsenic. Environ. Sci. Technol. 53, 7288–7295. https://doi.org/10.1021/acs.est.8b06335.
Shangguan, Y., Qin, X., Zhao, L., Wang, L., Hou, H., 2016. Effects of iron oxide on antimony (V) adsorption in natural soils: transmission electron microscopy and X-ray photoelectron spectroscopy measurements. J. Soils Sediments 16, 509–517. https://doi.org/10.1007/s11368-015-1229-9.
Sherman, D.M., Randall, S.R., 2003. Surface complexation of arsenic(V) to iron(III) (hydr)oxides: structural mechanism from ab initio molecular geometries and EXAFS spectroscopy. Geochim. Cosmochim. Acta 67, 4223–4230. https://doi.org/10.1016/S0016-7037(03)00237-0.
Smith, L.M., Maher, W.A., Craig, P.J., Jenkins, R.O., 2002. Speciation of volatile antimony compounds in culture headspace gases ofCryptococcus humicolus using solid phase microextraction and gas chromatography-mass spectrometry. Appl. Organometal. Chem. 16, 287–293. https://doi.org/10.1002/aoc.303.
Szopka, K., Gruss, I., Gruszka, D., Karczewska, A., Gediga, K., Gałka, B., Dradrach, A., 2021. The effects of forest litter and waterlogging on the ecotoxicity of soils strongly enriched in arsenic in a historical mining site. Forests 12, 355. https://doi.org/10.3390/f12030355.
Takahashi, Y., Minamikawa, R., Hattori, K.H., Kurishima, K., Kihou, N., Yuita, K., 2004. Arsenic behavior in Paddy fields during the cycle of flooded and non-flooded periods. Environ. Sci. Technol. 38, 1038–1044. https://doi.org/10.1021/es034383n.
Talukder, A.S.M.H.M., Meisner, C.A., Sarkar, M.A.R., Islam, M.S., Sayre, K.D., Duxbury, J.M., Lauren, J.G., 2012. Effect of water management, arsenic and phosphorus levels on rice in a high-arsenic soil–water system: II. Arsenic uptake. Ecotoxicology and Environmental Safety 80, 145–151. https://doi.org/10.1016/j.ecoenv.2012.02.020.
Tandy, S., Hockmann, K., Keller, M., Studer, B., Papritz, A., Schulin, R., 2018. Antimony mobility during prolonged waterlogging and reoxidation of shooting range soil: a field experiment. Sci. Total Environ. 624, 838–844. https://doi.org/10.1016/j.scitotenv.2017.12.193.
Tang, X., Zou, L., Su, S., Lu, Y., Zhai, W., Manzoor, M., Liao, Y., Nie, J., Shi, J., Ma, L.Q., Xu, J., 2021. Long-term manure application changes bacterial communities in Rice rhizosphere and arsenic speciation in Rice grains. Environ. Sci. Technol. 55, 1555–1565. https://doi.org/10.1021/acs.est.0c03924.
Tella, M., Pokrovski, G.S., 2008. Antimony(V) complexing with O-bearing organic ligands in aqueous solution: an X-ray absorption fine structure spectroscopy and potentiometric study. Mineral. Mag. 72, 205–209. https://doi.org/10.1180/minmag.2008.072.1.205.
Tella, M., Pokrovski, G.S., 2009. Antimony(III) complexing with O-bearing organic ligands in aqueous solution: an X-ray absorption fine structure spectroscopy and solubility study. Geochim. Cosmochim. Acta 73, 268–290. https://doi.org/10.1016/j.gca.2008.10.014.
Thayer, J.S., 2002. Review: biological methylation of less-studied elements. Appl. Organometal. Chem. 16, 677–691. https://doi.org/10.1002/aoc.375.
Tian, H., Zhou, J., Zhu, C., Zhao, D., Gao, J., Hao, J., He, M., Liu, K., Wang, K., Hua, S., 2014. A comprehensive global inventory of atmospheric antimony emissions from anthropogenic activities, 1995–2010. Environ. Sci. Technol. 48, 10235–10241. https://doi.org/10.1021/es405817u.
Tighe, M., Lockwood, P., Wilson, S., 2005. Adsorption of antimony(v) by floodplain soils, amorphous iron(iii) hydroxide and humic acid. J. Environ. Monit. 7, 1177. https://doi.org/10.1039/b508302h.
Upadhyay, M.K., Majumdar, A., Suresh Kumar, J., Srivastava, S., 2020. Arsenic in rice agroecosystem: solutions for safe and sustainable Rice production. Front. Sustain. Food Syst. 4, 53. https://doi.org/10.3389/fsufs.2020.00053.
USDA, 1987. USDA Soil Textural Classification.pdf.
Vahter, M., Concha, G., 2001. Role of metabolism in arsenic toxicity. Pharmacol. Toxicol. 89, 1–5. https://doi.org/10.1034/j.1600-0773.2001.d01-128.x.
Van Vleek, B., Amarasiriwardena, D., Xing, B., 2011. Investigation of distribution of soil antimony using sequential extraction and antimony complexed to soil-derived humic acids molar mass fractions extracted from various depths in a shooting range soil. Microchem. J. 97, 68–73. https://doi.org/10.1016/j.microc.2010.05.015.
Verbeeck, M., Warrinnier, R., Gustafsson, J.P., Thiry, Y., Smolders, E., 2019. Soil organic matter increases antimonate mobility in soil: an Sb(OH)6 sorption and modelling study. Appl. Geochem. 104, 33–41. https://doi.org/10.1016/j.apgeochem.2019.03.012.
Vithanage, M., Rajapaksha, A.U., Dou, X., Bolan, N.S., Yang, J.E., Ok, Y.S., 2013. Surface complexation modeling and spectroscopic evidence of antimony adsorption on iron-oxide-rich red earth soils. J. Colloid Interface Sci. 406, 217–224. https://doi.org/10.1016/j.jcis.2013.05.053.
Vriens, B., Ammann, A.A., Hagendorfer, H., Lenz, M., Berg, M., Winkel, L.H.E., 2014a. Quantification of methylated selenium, sulfur, and arsenic in the environment. PLoS ONE 9, e102906. https://doi.org/10.1371/journal.pone.0102906.
Vriens, B., Lenz, M., Charlet, L., Berg, M., Winkel, L.H.E., 2014b. Natural wetland emissions of methylated trace elements. Nat. Commun. 5, 3035. https://doi.org/10.1038/ncomms4035.
Wan, X., Tandy, S., Hockmann, K., Schulin, R., 2013a. Changes in sb speciation with waterlogging of shooting range soils and impacts on plant uptake. Environ. Pollut. 172, 53–60. https://doi.org/10.1016/j.envpol.2012.08.010.
Wan, X., Tandy, S., Hockmann, K., Schulin, R., 2013b. Effects of waterlogging on the solubility and redox state of sb in a shooting range soil and its uptake by grasses: a tank experiment. Plant Soil 371, 155–166. https://doi.org/10.1007/s11104-013-1684-2.
Wang, S., Mulligan, C.N., 2006. Effect of natural organic matter on arsenic release from soils and sediments into groundwater. Environ. Geochem. Health 28, 197–214. https://doi.org/10.1007/s10653-005-9032-y.
Wang, X., He, M., Xie, J., Xi, J., Lu, X., 2010. Heavy metal pollution of the world largest antimony mine-affected agricultural soils in Hunan province (China). J. Soils Sediments 10, 827–837. https://doi.org/10.1007/s11368-010-0196-4.
Wang, X., He, M., Xi, J., Lu, X., 2011. Antimony distribution and mobility in rivers around the world's largest antimony mine of xikuangshan, Hunan Province, China. Microchem. J. 97, 4–11. https://doi.org/10.1016/j.microc.2010.05.011.
Weber, F.-A., Voegelin, A., Kaegi, R., Kretzschmar, R., 2009a. Contaminant mobilization by metallic copper and metal sulphide colloids in flooded soil. Nature Geosci 2, 267–271. https://doi.org/10.1038/ngeo476.
Weber, F.-A., Voegelin, A., Kretzschmar, R., 2009b. Multi-metal contaminant dynamics in temporarily flooded soil under sulfate limitation. Geochim. Cosmochim. Acta 73, 5513–5527. https://doi.org/10.1016/j.gca.2009.06.011.
Wehmeier, S., Feldmann, J., 2005a. Investigation into antimony mobility in sewage sludge fermentation. J. Environ. Monit. 7, 1194. https://doi.org/10.1039/b509538g.
Wehmeier, S., Raab, A., Feldmann, J., 2004. Investigations into the role of methylcobalamin and glutathione for the methylation of antimony using isotopically enriched antimony (V). Appl. Organometal. Chem. 18, 631–639. https://doi.org/10.1002/aoc.692.
Wickenheiser, E.B., Michalke, K., Hensel, R., Drescher, C., Hirner, A., Rutishauser, B., Bachofen, R., 1998. Volatile Compounds in Gases Emitted From Wetland Bogs Near Lake Cadagno.
Wilson, S.C., Lockwood, P.V., Ashley, P.M., Tighe, M., 2010. The chemistry and behaviour of antimony in the soil environment with comparisons to arsenic: a critical review. Environ. Pollut. 158, 1169–1181. https://doi.org/10.1016/j.envpol.2009.10.045.
World Health Organization, 2003. Antimony in drinking water. Guidelines for Drinking-Water Quality.
Wu, T.-L., Cui, X.-D., Cui, P.-X., Ata-Ul-Karim, S.T., Sun, Q., Liu, C., Fan, T.-T., Gong, H., Zhou, D.-M., Wang, Y.-J., 2019. Speciation and location of arsenic and antimony in rice samples around antimony mining area. Environ. Pollut. 252, 1439–1447. https://doi.org/10.1016/j.envpol.2019.06.083.
Xia, B., Yang, Y., Li, F., Liu, T., 2022. Kinetics of antimony biogeochemical processes under pre-definite anaerobic and aerobic conditions in a paddy soil. J. Environ. Sci. 113, 269–280. https://doi.org/10.1016/j.jes.2021.06.009.

Xiang, L., Liu, C., Liu, D., Ma, L., Qiu, X., Wang, H., Lu, X., 2022. Antimony transformation and mobilization from stibnite by an antimonite oxidizing bacterium bosea sp. AS-1. J. Environ. Sci. 111, 273–281. https://doi.org/10.1016/j.jes.2021.03.042.

Xu, X., Chen, C., Wang, P., Kretzschmar, R., Zhao, F.-J., 2017. Control of arsenic mobilization in paddy soils by manganese and iron oxides. Environ. Pollut. 231, 37–47. https://doi.org/10.1016/j.envpol.2017.07.084.

Yamaguchi, N., Nakamura, T., Dong, D., Takahashi, Y., Amachi, S., Makino, T., 2011. Arsenic release from flooded paddy soils is influenced by speciation, eh, pH, and iron dissolution. Chemosphere 83, 925–932. https://doi.org/10.1016/j.chemosphere.2011.02.044.

Yan, H., Wang, X., Yang, Y., Duan, G., Zhang, H., Cheng, W., 2020. The effect of straw-returning on antimony and arsenic volatilization from paddy soil and accumulation in rice grains. Environ. Pollut. 263. https://doi.org/10.1016/j.envpol.2020.114581.

Yan, M., Zeng, X., Wang, J., Meharg, A.A., Meharg, C., Tang, X., Zhang, L., Bai, L., Zhang, J., Su, S., 2020. Dissolved organic matter differentially influences arsenic methylation and volatilization in paddy soils. J. Hazard. Mater. 388, 121795. https://doi.org/10.1016/j.jhazmat.2019.121795.

Yang, H., He, M., 2016. Distribution and speciation of selenium, antimony, and arsenic in soils and sediments around the area of xikuangshan (China): soil. Clean Soil Air Water 44, 1538–1546. https://doi.org/10.1002/clen.201400522.

Yang, H., He, M., Wang, X., 2015. Concentration and speciation of antimony and arsenic in soil profiles around the world's largest antimony metallurgical area in China. Environ. Geochem. Health 37, 21–33. https://doi.org/10.1007/s10653-014-9627-2.

Yang, S., Zhai, W., Tang, X., Gustave, W., Yuan, Z., Guo, T., Shu, Y., 2021. The effect of manure application on arsenic mobilization and methylation in different paddy soils. Bull. Environ. Contam. Toxicol. https://doi.org/10.1007/s00128-021-03317-1.

Ye, L., Meng, X., Jing, C., 2020. Influence of sulfur on the mobility of arsenic and antimony during oxic-anoxic cycles: differences and competition. Geochim. Cosmochim. Acta 288, 51–67. https://doi.org/10.1016/j.gca.2020.08.007.

Zhou, J., Nyirenda, M.T., Xie, L., Li, Y., Zhou, B., Zhu, Y., Liu, H., 2017. Mine waste acidic potential and distribution of antimony and arsenic in waters of the xikuangshan mine, China. Appl. Geochem. 77, 52–61. https://doi.org/10.1016/j.apgeochem.2016.04.010.

Zhou, S., Hursthouse, A., Chen, T., 2019. Pollution characteristics of Sb, As, Hg, Pb, Cd, and Zn in soils from different zones of Xikuangshan antimony mine. J. Anal. Methods Chem. 2019, 1–9. https://doi.org/10.1155/2019/2754385.